

Charles University
Faculty of Science
Department of Physical and Macromolecular Chemistry



Doctoral thesis

Use of Ionic liquids for preparation of epoxy materials

M.Sc. Marwa Rebei

Study programme: Macromolecular Chemistry

Supervisor: Ing. Hynek Beneš, Ph.D.

Institute of Macromolecular Chemistry of the Czech Academy of Sciences
Department of Polymer Processing



INSTITUTE OF
MACROMOLECULAR
CHEMISTRY

Prague 2024

Univerzita Karlova
Přírodovědecká fakulta
Katedra fyzikální a makromolekulární chemie



Disertační práce
Využití iontových kapalin pro přípravu epoxidů

M.Sc. Marwa Rebei
Studijní program: Makromolekulární chemie

Školitel: Ing. Hynek Beneš, Ph.D.

Ústav makromolekulární chemie AV ČR, v. v. i.
Oddělení: Zpracování polymerních materiálů



Praha 2024

Declaration

Hereby, I declare that I have written this doctoral independently under the supervision of Ing. Hynek Beneš, PhD., and all the resources used here, have been appropriately cited, to the best of my knowledge. This work has not been submitted to obtain any other degree, diploma or academic qualification.

Prague, 17th of May 2024

Marwa Rebei

*To my father
who would have been proud*

Acknowledgement

Initially, I would like to express my gratitude to the Institute of Macromolecular Chemistry CAS (IMC) for providing me with research facilities and extensive knowledge in the field of polymer chemistry. I am also grateful to the Faculty of Sciences of Charles University for enabling me to pursue my doctoral studies and fulfil my aspirations, and to the Grant Agency of Charles University for financially supporting my GAUK project No. 4130022.

This journey would not have been possible without the assistance and encouragement of certain individuals. Therefore, it is important for me to express my gratitude, first of all, to my Ph.D supervisor, Ing. Hynek Beneš, Ph.D., for his guidance, constant advice, and support throughout these years. In addition, I am grateful to my informal advisor, Dr. Ricardo Keitel Donato, for his invaluable consultations throughout my thesis work.

I am grateful of the opportunity to conduct my research at the Department of Polymer Processing at IMC, where I received assistance and support from my kind colleagues and lab mates not only in work aspects but also in informal Czech language lessons. I am also grateful to have met many kind and helpful people at IMC, with whom I have formed friendships that I cherish. Thank you all for making the last 5 years very enjoyable.

Finally, I would like to express my love and gratitude to my family, my mother, my brothers, and my life partner, for being the source of comfort, strength, and courage. Without their support, I wouldn't have the strength and motivation to pursue this dream.

Table of Contents

Abstract	13
Abstrakt	15
List of symbols	18
1. Introduction	19
1.1. Ring-opening polymerization of epoxy monomer	19
1.2. Epoxy network formation.....	22
1.3. Ionic liquids for epoxy polymerization	23
1.3.1. Initiative/catalytic properties of ionic liquids in epoxy polymerization	24
1.3.2. Ionic liquids for epoxy - CO ₂ cycloaddition.....	25
1.3.3. Effect of ionic liquids on properties of epoxy networks.....	27
2. Aims of the thesis	28
3. Experimental part	29
4. Results and discussion.....	32
4.1. Epoxy-dicarboxylic acid copolymerization reaction.....	32
4.1.1. Catalytic properties of ionic liquid in epoxy-dicarboxylic acid copolymerization ..	32
4.1.2. Proposed mechanism of epoxy-acid ring-opening polymerization mediated by imidazolium-based ionic liquid.....	36
4.1.3. Thermomechanical properties of the cured epoxy-dicarboxylic acid networks ...	38
4.2. Epoxy-anhydride copolymerization reaction	39
4.2.1. Catalytic activity of metal-based ionic liquids in the epoxy-anhydride copolymerization	39
4.2.2. Mechanism investigation of the epoxy-anhydride copolymerization.....	42
4.2.3. Optimization of the content of metal ionic liquids	46
4.2.4. Final thermal and mechanical properties of the optimized epoxy-anhydride networks.....	47
4.3. Epoxy-CO ₂ cycloaddition reaction.....	49
4.3.1. Catalytic properties of ionic liquids in CO ₂ -epoxy cycloaddition reaction	49
4.3.2. Study of the CO ₂ -epoxy cycloaddition reaction mechanism initiated by ionic liquid	52
4.3.3. Synthesis of non-isocyanate polyurethanes from CO ₂ -epoxy: proof of concept..	53
5. Conclusion.....	56
Publications	57
Conference contributions	58
Grants and projects.....	58
Appendices: Publications included in this thesis	59
References	60

Abstract

Epoxy resins represent an important category of thermosets widely as coatings, electronic encapsulants, matrices for composites, etc., due to their beneficial properties, such as strong adhesion, high chemical and electrical resistance, and good processability. However, their curing reactions present some limitations, such as using catalysts (for example, organometallics, complexes and MOFs) which are active at high reaction temperatures. In most cases, these catalysts are toxic and require organic solvents. Consequently, alternative non-toxic catalysts/initiators that can promote well-controlled fast curing under mild conditions have been explored while maintaining sufficient thermomechanical properties of the formed epoxy networks.

In this thesis, three different epoxy ring opening reactions induced by various imidazolium ionic liquids (ILs) were studied.

The first subsection (4.1) discusses the step-growth epoxy-dicarboxylic acid polymerization in an imidazolium IL medium conducted under mild conditions ($T = 80\text{--}120\text{ }^{\circ}\text{C}$). The IL was shown to act as both a solvent and an initiator/catalyst for the reaction. In addition, IL-anions (chloride, bis(trifluoromethylsulfonyl) imide, or methanesulfonate) strongly affect the progress of the reaction. It was found that the Cl^- anion is the most effective epoxy ring-opening initiator, suitable for the production of glassy epoxy networks.

In the second subsection (4.2), the epoxy-anhydride copolymerization in the presence of imidazolium metal-containing ILs (MILs), bearing tetra-chlorinated iron, cobalt or zinc, and imidazolium metal-free, 1-butyl-3-methylimidazolium chloride (BMIMCl) is investigated. It was observed that MILs significantly accelerated epoxy-anhydride cross-link reaction more than the metal-free BMIMCl, especially at low temperatures, due to MILs' ability to activate a rapid anhydride ring opening resulting in the formation of carboxyl groups, that initiated further polyesterification. Despite various MILs-initiated pathways (polyesterification, imidazole and counter-anion), the alternating epoxy-anhydride copolymer chain was formed. Finally, MILs-induced crosslinking resulted in homogeneous network build-up producing glassy thermoset materials with increased cross-link density, a high glass transition temperature and excellent thermal stability.

The last subsection (4.3) describes the cycloaddition reaction between carbon dioxide (CO_2) and epoxy monomer in the presence of BMIMCl, and MILs, which showed the anionic

Cl⁻ initiation of the oxirane ring. The ILs used promoted fast and high yields of cyclic carbonates (up to 99% within 1 h). The subsequent aminolysis of the cyclic carbonates with a monofunctional amine led to the conversion into β -hydroxyurethanes without using an additional catalyst.

It has been demonstrated that ILs can be considered as novel additives for various epoxy systems enabling, the epoxy ring opening, the epoxy crosslinking with functional compounds, and the CO₂ absorption and cycloaddition to epoxy.

Abstrakt

Epoxidové pryskyřice představují důležitou skupinu reaktoplastů, široce používaných jako nátěrové hmoty, licí pryskyřice v elektronice, matrice strukturních kompozitů atd., a to díky svým výhodným vlastnostem, jako je silná adheze, vysoká chemická a elektrická odolnost a dobrá zpracovatelnost. Nevýhodou jsou jejich nároky na vytvrzování, související s dlouhými vytvrzovacími cykly a potřebou specifických katalyzátorů (například organokovové sloučeniny a komplexy či využití tzv. metal-organic framework, MOF, struktur), které jsou dostatečně aktivní až při vysokých reakčních teplotách. Ve většině případů jsou tyto katalyzátory toxické či vyžadují použití organických rozpouštědel. V důsledku toho jsou zkoumány alternativní netoxické katalyzátory/iniciátory, které podporují dobře kontrolovatelné a rychlé vytvrzování za mírných podmínek, a přitom vedou k vytvoření kovalentních sítí s vynikajícími termomechanickými vlastnostmi.

V této práci byly studovány tři různé reakce otevření epoxidového kruhu vyvolané různými typy imidazoliových iontových kapalin.

První kapitola (4.1) pojednává o stupňovité polymeraci mezi epoxidovou pryskyřicí a dikarboxylovou kyselinou v přítomnosti imidazoliových iontových kapalin, která se prováděla za mírných podmínek ($T = 80\text{--}120\text{ }^{\circ}\text{C}$). Bylo prokázáno, že iontová kapalina působí jako rozpouštědlo a zároveň iniciátor/katalyzátor reakce. Kromě toho anionty iontových kapalin, chlorid, bis(trifluoromethylsulfon)imid, nebo methanesulfonát, silně ovlivňují průběh reakce. Bylo zjištěno, že chloridový anion je nejúčinnějším iniciátorem otevření epoxidového kruhu, který lze využít pro tvorbu sklovitých epoxidových sítí.

Ve druhé kapitole (4.2) je zkoumána řetězová kopolymerace epoxidové pryskyřice a cyklického anhydridu za přítomnosti imidazoliových iontových kapalin obsahující ve struktuře aniontu koordinované kovy (železo, kobalt a zinek) tak inekovové imidazoliové iontové kapaliny (1-butyl-3-methylimidazoliumchloridu, BMIMCl). Bylo pozorováno, že kovové iontové kapaliny významně urychlily reakci epoxid-anhydrid, zejména při nízkých teplotách, a to díky jejich schopnosti aktivovat rychlou hydrolyzu anhydridového kruhu. To vedlo k tvorbě karboxylových skupin, které iniciovaly další polyesterifikaci. Přes různé způsoby iniciace (kromě výše uvedené polyesterifikace, probíhala iniciace i tzv. imidazolovou cestou a iniciací anionem iontové kapaliny) docházelo u vznikajícího polymerního řetězce vždy k vytvoření alternujícího sekvenčního uspořádání monomerních jednotek. Tímto způsobem lze připravit

vysoce homogenní sklovité epoxidové sítě, které vykazovaly vysokou síťovou hustotu, teplotu skelného přechodu a vynikající termickou stabilitu.

Poslední kapitola (4.3) popisuje cykloadiční reakci mezi epoxidovým monomerem a oxidem uhličitým za přítomnosti kovových iontových kapalin a BMIMCl, které skrz svůj anion iniciují otevírání oxiranového kruhu. Testované iontové kapaliny vedou k poměrně rychlé konverzi epoxidu a vysokým výtěžkům vznikajících cyklických karbonátů (až 99 % během 1 h). Následnou aminolýzou cyklických karbonátů pomocí monofunkčního aminu se podařilo připravit β -hydroxyurethany, a to bez použití dalších katalyzátorů.

Bylo prokázáno, že imidazoliové iontové kapaliny lze považovat za perspektivní přísady do epoxidových systémů, a to vzhledem k jejich schopnosti iniciovat otevření epoxidového kruhu, a katalyzovat jeho adiční reakce s dalšími sloučeninami.

List of abbreviations

1IP	One ion pair
1MIM	1-Methylimidazole
2IP	Two ion pairs
BA	<i>n</i> -Butylamine
BMIMCl	1-Butyl-3-methylimidazolium chloride
BMIMMeS	1-Butyl-3-methylimidazolium methansulfonate
BMIMNTf ₂	1-Butyl-3-methylimidazolium bis(trifluoromethylsulfonyl) imide
CO ₂	Carbon dioxide
DFT	Density Functional Theory
DGEBA	Bisphenol A diglycidyl ether
DGEMHQ	2,2'-[(2-methoxy-1,4-phenylene)bis(oxyethylene)] bis(oxirane)
DMTA	Dynamic mechanical and thermal analysis
DSC	Differential scanning calorimetry
Expl.	Explicit solvation
FTIR	Fourier-transform infrared spectroscopy
IL(s)	Ionic liquid(s)
Impl.	Implicit solvation
INT	Intermediates
MALDI-TOF MS	Matrix-assisted laser desorption/ionization-time of flight mass spectrometry
MCl ₄	Tetrachlorinated metal
MHHPA	Hexahydro-4-methylphthalic anhydride
MIL(s)	Metal-based ionic liquid(s)
NIPUs	Non-isocyanate polyurethanes
NIR	Near-infrared spectroscopy
NMR	Nuclear magnetic resonance
Nu ⁻	Nucleophile
PGE	Phenyl glycidyl ether
PROD	Products
REAC	Reactants
ROP	Ring-opening polymerization
SA	Succinic acid
TGA	Thermogravimetric analysis
TS1	Transition state 1
TS2	Transition state 2
VOC(s)	Volatile organic compound(s)

List of symbols

α_{DSC}	Epoxy conversion from DSC
G'	Storage modulus
M_c	Molecular weight between crosslinks
M_w	Molecular weight
$\tan \delta$	Loss factor
T_d	Decomposition temperature
T_{d10}	Decomposition temperature at 10% of mass loss
$T_{d5\%}$	Decomposition temperature at 5% of mass loss
T_g	Glass transition temperature
T_m	Melting temperature
T_{max}	Maximal mass loss / Temperature at the maximum curing exotherm
T_{onset}	Onset temperature
T_α	Alpha transition temperature at the maximum of the $\tan \delta$ peak
α_{FTIR}	Conversion calculated from FTIR spectra
α_{NMR}	Conversion calculated from NMR spectra
ΔH_r	Enthalpy of the reaction
$\Delta H_{r, total}$	Total reaction heat
ν_e	Crosslink density

1. Introduction

For decades, epoxy resins have been one of the most important categories of thermosets, widely used in civil infrastructure, automotive industry, aerospace, and aeronautical technologies, due to their promising properties, such as strong adhesion, high chemical and electrical resistance, and good processability [1–4]. In general, epoxy thermosets are formed from a liquid mixture of monomers containing multifunctional epoxy (oxirane rings) resins that can react with each other or with other functional compounds such as amines, anhydrides, acids or alcohols to form a polymer network [5]. To prepare a chemically (covalently) crosslinked epoxy network, it is essential to use an initiator or catalyst to promote the opening of the oxirane ring which can further react with another functional compound. The most commonly used catalysts are nitrogen-containing compounds, such as polyamines and dicyanamide that can also play the role of a hardener, or imidazole compounds [3,6], and metal complexes (such as zinc or cobalt complexes) [7]. However, these conventional catalysts are typically used in large quantities, are only active at high reaction temperatures, are not recyclable, and are often solids with low solubility in epoxy monomers, requiring the addition of organic solvents [8]. These drawbacks present current challenges in the epoxy curing processes in terms of environmental and sustainability issues. Therefore, there is nowadays an increasing interest to exploit more environmentally friendly epoxy curing conditions while using recyclable and less toxic catalysts, without the need for solvents or volatile organic compounds (VOCs), which can contribute to a more sustainable chemistry [9,10]. In this context, ionic liquids (ILs) seem to be a promising class of epoxy catalysts/additives due to their low melting point and viscosity as well as their versatile chemical structures that allow tuning the miscibility with the epoxy monomers [11–14]. Recent studies have shown their catalytic ability in epoxy polymerizations at low reaction temperatures, without additional solvents, along with potential recyclability at the end of the reaction [15–20].

1.1. Ring-opening polymerization of epoxy monomer

Diglycidyl ether of bisphenol A (DGEBA) is, by far, the most commonly used epoxy monomer (resin). DGEBA is synthesized from bis(4-hydroxyphenylene)-2,2 propane (bisphenol A) and 1-chloroprene-2-oxide (epichlorohydrin) in the presence of sodium hydroxide [21]. Epoxy resins can contain aromatic, cycloaliphatic or aliphatic structures and various numbers of oxirane groups. They can be polymerized by homopolymerization (with the addition of an initiator) or copolymerization (with the addition of co-monomer, called

“hardener”) [22]. Fig. 1 depicts a schematic illustration of typical ways in which the epoxy monomers can be polymerized.

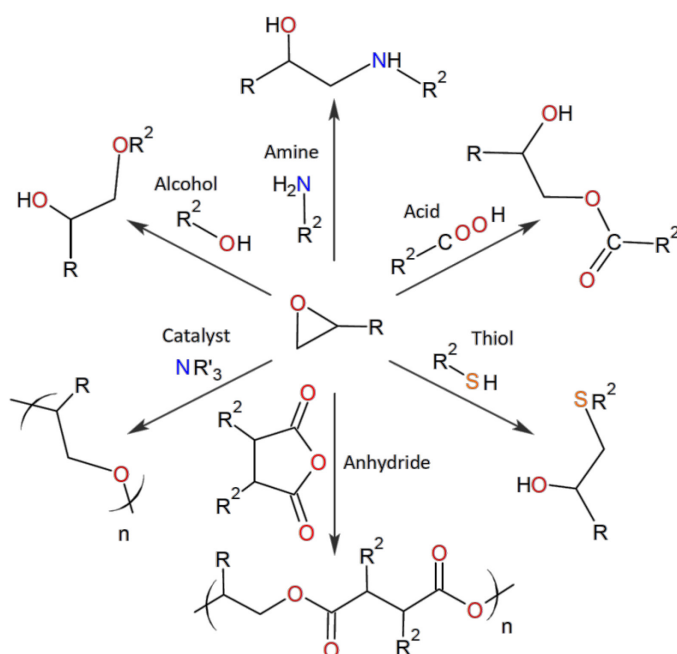


Fig. 1. Possible polymerization routes for epoxy resins.

Epoxy polymers can be prepared by step or chain growth polymerization, or by a combination of both mechanisms [21]. Step-growth polymerization is characterized by a stepwise sequence of reactions between reactive sites, and each step results in the disappearance of two co-reacting sites and the formation of a covalent bond between two functional groups [21]. On the other hand, chain growth polymerization proceeds through three main steps, initiation, propagation, chain transfer, and termination. It is characterized by the formation of active centers (anion or cation) that generate primary chains through the consecutive addition of monomers during the propagation step. Since active centers are always present at the end of the polymer chain, the propagation proceeds until it is interrupted by a chain transfer or termination step [21]. Epoxy-amine and epoxy-acid polymerization are typical reactions of step-growth polymerization, while epoxy-anhydride follows chain-growth polymerization (Fig. 1).

The chain-growth ring-opening polymerization (ROP) of epoxides can occur via *i*) cationic homopolymerization, *ii*) anionic, or *iii*) coordination mechanisms. The cationic homopolymerization of epoxides is initiated by electrophiles, such as inorganic halogens, organometallics, protonated acids, or organic salts [21]. Fig. 2(A) shows a typical cationic homopolymerization of an epoxide via end-chain activation [7]. The initiation step involves an electrophilic attack on the oxygen of the oxirane ring resulting in an oxonium ion. Another

epoxide can then attack either on the least hindered carbon of the oxonium ion (Fig. 2(A), pathway 1) or on the carbon attached to the -R end group (Fig. 2(A), pathway 2). The anionic polymerization involves a nucleophilic attack on the least hindered carbon of the oxirane ring [6,23–25]. Due to the high reactivity of the oxirane ring towards the nucleophiles, the reaction leads to the rapid formation of a polyether chain. The ROP of epoxy monomer via a nucleophile (Nu^-) is illustrated in Fig. 2(B).

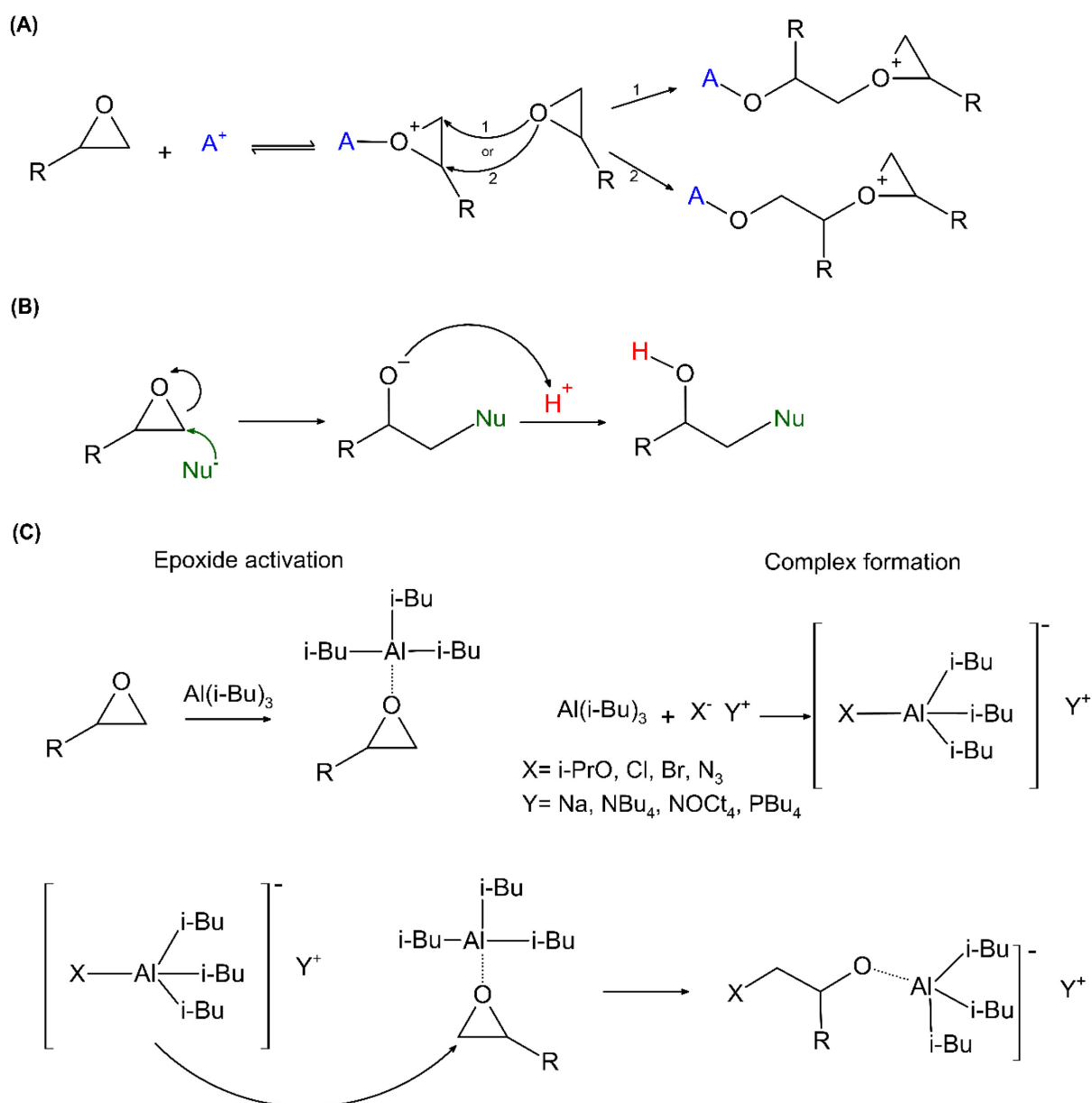


Fig. 2. ROP of epoxy resin via (A) cationic homopolymerization route (B) anionic nucleophilic route, and (C) coordination route. Reproduced from [7,23,26].

The coordination ROP of epoxides aims to achieve high molecular weights of polyethers (e.g. polyethylene oxide). The most commonly used catalysts for this type of polymerization

are characterized by mild nucleophilicity and high Lewis acidity, e.g. derivatives of divalent and trivalent metals (Ca, Zn, and Al) [7,26]. The initiation mechanism of epoxides via the coordination polymerization is based on an activated monomer strategy, where, for example, a trialkyl aluminium compound is combined with an organic salt to improve the initiation system (Fig. 2(C)).

1.2. Epoxy network formation

The epoxy monomers used to generate a polymer network contain two or more oxirane groups per molecule. A covalent epoxy network is created when at least one of the monomers (an epoxy resin and eventually a hardener) involved in the reaction has a functionality higher than two [10,22,27]. Two macroscopic phenomena occur during the epoxy network build-up: gelation and vitrification [28]. During the gelation process, a three-dimensional polymer network is formed and the average molecular weight tends to infinity resulting in a giant macromolecular structure that percolates the reaction medium (Fig. 3) [5,21,29].

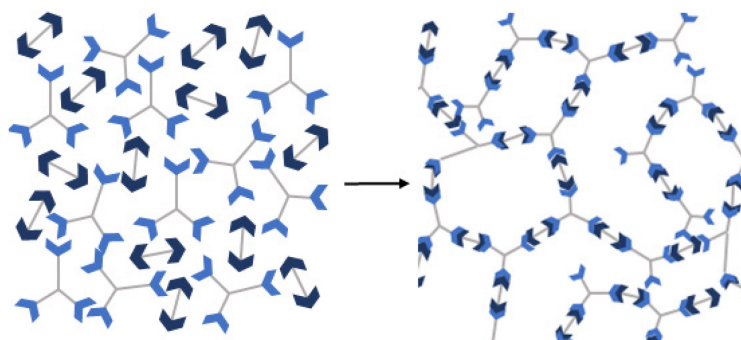


Fig. 3. Schematic representation of the gelation transition between tri- and di-functional monomers in a step polymerization. Reproduced from [30].

In the following post-gel phase, both the crosslink density (ν_e) and elastic modulus increase while the soluble fraction of the polymer, known as the sol fraction, decreases. Since the local mobility of the functional groups is not affected by gelation, the kinetics of the crosslinking reaction does not change after the gelation point is reached.

During polymerization, when the glass transition temperature of the reactive system (T_g) becomes higher than the curing temperature, T ($T_g \geq T$), the vitrification phenomenon occurs. The vitrification may occur before or after the gelation and is therefore characterized by the transition from a liquid or a gel to a glassy state [21,28,31]. Since the vitrification results in a reduced mobility of the chain segments and/or unreacted functional groups, the crosslinking becomes slower and diffusion-controlled [5,30].

1.3. Ionic liquids for epoxy polymerization

Ionic liquids (ILs) are organic molten salts in the liquid state and are distinguished by a low melting point (below 100 °C). Unlike inorganic salts, which require a solvent to dissociate into ion pairs, ILs do not require solvation because they exist as dissociated ion pairs at room temperature. Their specific structure is composed of a cation and an anion, which allows the destabilization of solid-phase crystals, and hence, they are often liquid at ambient temperatures [32,33]. The tuneable structure of IL leads to a wide range of possible anion–cation combinations by balancing the ion–ion interactions and symmetry. For instance, the cationic moiety could be ammonium, phosphonium, or imidazolium, and the anion could include halides, formate, nitrate, imide, or thiocyanate, as illustrated in Fig. 4(a,b).

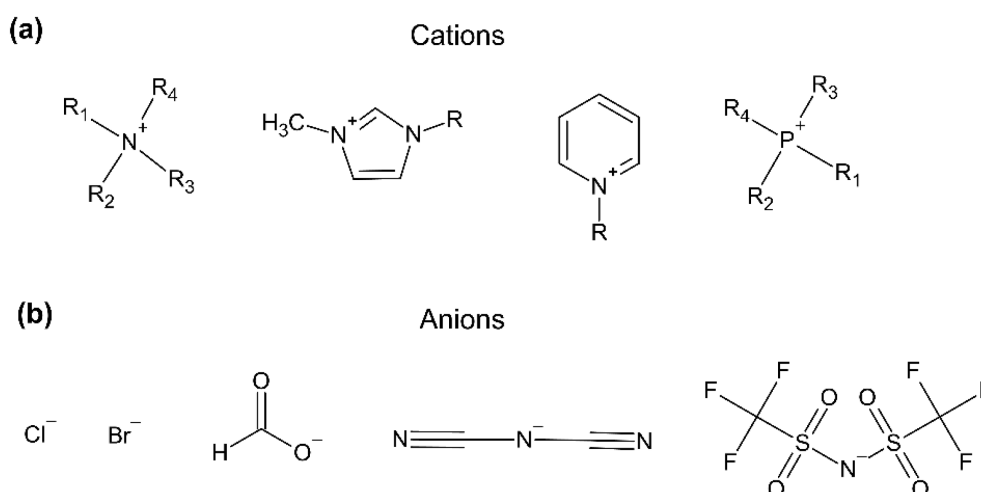


Fig. 4. Structures of commonly used (a) cations (from left to right: tetraalkylammonium, 1-methyl-3-alkylimidazolium, 1-alkyl pyridinium, tetraalkylphosphonium) and (b) anions (from left to right: chloride, bromide, formate, dicyanamide, bis(trifluoromethylsulfonyl)imide) in the synthesis of ILs. Reproduced from [32].

ILs are also characterized by other outstanding properties such as high thermal and chemical stability, low vapor pressure, tuneable physicochemical properties, and low flammability [32–35]. Thus, they are usually considered as “green” solvents, catalysts, reagents, initiators, or even multifunctional additives in many chemical processes, such as the catalytic conversion of cellulose into value-added chemicals and fuel products, thermoregulated catalytic systems in which temperature-responsive ILs are used [36], and several important oxidation reactions [37]. Furthermore, ILs are compatible with many polymers and monomers, making them perfect candidates as additives, catalysts, and initiators for various polymerization reactions [33,38–40].

1.3.1. Initiative/catalytic properties of ionic liquids in epoxy polymerization

The behaviour of ILs can vary largely depending on the functional group attached to the cation or anion, which makes them acidic, basic, or organocatalytic compounds [41]. The acidic nature of Lewis and Brønsted acid ILs has been shown to provide effective and reusable catalysts for many polymerization reactions [41,42]. Perchacz et al. [43] found that Brønsted-acidic imidazolium ILs can catalyze coupling reactions between carboxyl groups and monofunctional epoxy monomer (Phenyl glycidyl ether, PGE). The reactivity of these ILs was influenced by varying the number of carboxyl groups and the steric properties of the cations and anions. These findings demonstrated that imidazolium ILs bearing carboxyl groups can serve as self-catalyzed “building blocks” for epoxy network build-up, facilitating the coupling reactions between the carboxyl and epoxy groups without necessity to use additional catalysts [43].

Binks et al. [44] suggested three possible mechanistic routes of epoxide ring opening induced by imidazolium ILs: a) the ‘carbene route’, due to the dissociation of the acidic proton of the imidazolium ring resulting in carbene formation, where a sufficient concentration of carbene compounds allows the initiation of epoxy ring opening, b) the ‘imidazole’ route, which occurs at temperatures approximately higher than 90 °C, where it originates from the dealkylation of the imidazolium ring, forming an N-heterocyclic carbon structure that attacks the least hindered epoxy carbon, and it appears to become more dominant with the increase of the IL’s concentration, and c) the counter ion route comprises the nucleophilic attack by the anion based on its nucleophilicity or basicity (Fig. 5(a-c)).

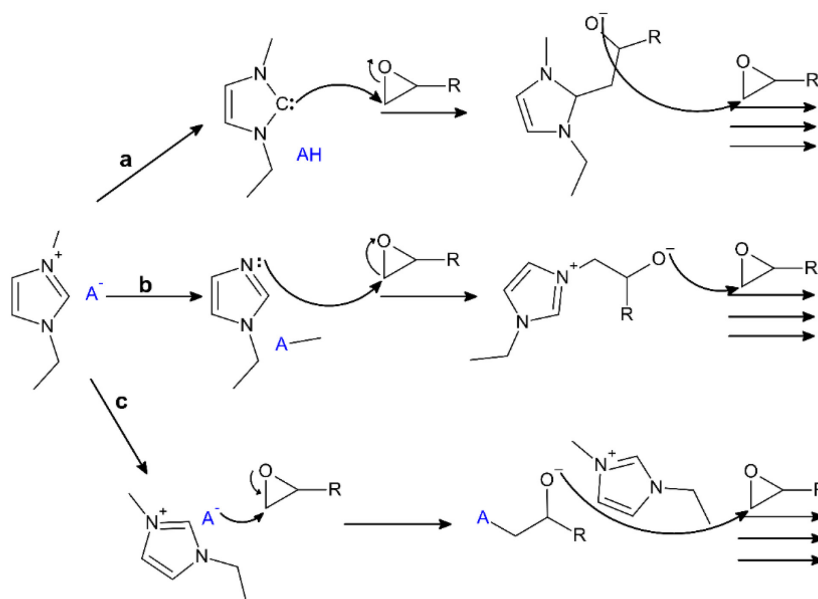


Fig. 5. Initiation pathways of epoxy polymerization reaction using imidazolium-based IL, via a) ‘carbene route’, b) imidazole route, and c) counter ion route. Reproduced from [44].

The use of imidazolium-based ILs as catalysts in epoxy polymerization offers several advantages. They operate under mild conditions, without using a solvent or co-catalyst [15,45]. In addition, ILs can be recovered and reused in further reactions, making them an environmentally friendly option for epoxy polymerization [12,13].

1.3.2. Ionic liquids for epoxy - CO₂ cycloaddition

ILs have been tested as catalysts for epoxy - CO₂ cycloaddition reactions aiming to produce cyclic carbonates [46–48] (Fig. 6(A)). This is mainly due to the high CO₂ solubility in ILs, which is dominantly influenced by the type of anion used, for example, (NTf₂⁻) anion showed a higher affinity for CO₂ absorption compared to (BF₄⁻) or (PF₆⁻) [49–53].

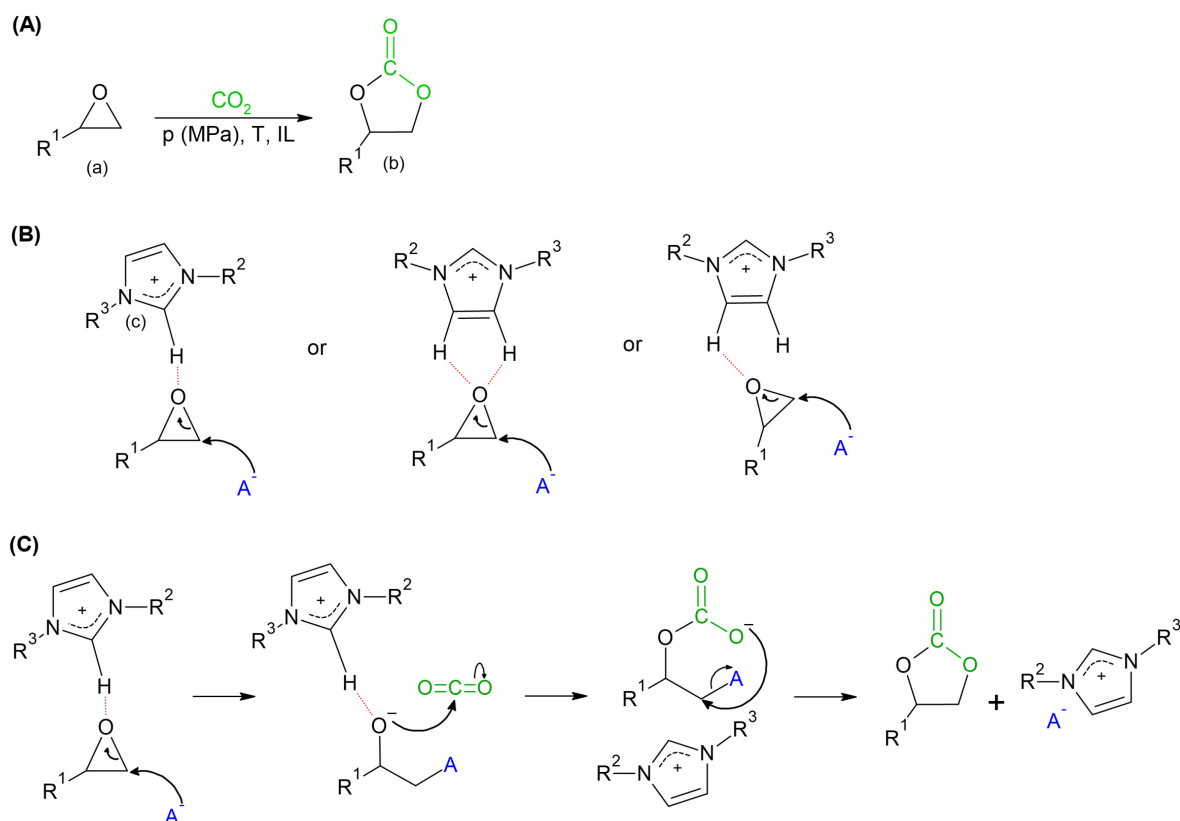


Fig. 6. (A) General CO₂ cycloaddition reaction to epoxy monomer to synthesize cyclic carbonate: (a) epoxy monomer, (b) monofunctional cyclic carbonate, (B) Possible H bonds between the oxirane ring and acidic proton in the imidazolium-ring, (C) Scheme of CO₂ cycloaddition mechanism to epoxy monomer via (c) imidazolium-based IL, with R¹= aromatic or aliphatic group, R² and R³=alkyl chains, and A⁻ = anion species. Reproduced from [54].

Recent studies have shown that different types of ILs, such as ammonium-based ILs [55,56], or phosphonium-based ILs [57] have yielded up to 99% of cyclic carbonates. Other studies demonstrated that functionalized imidazolium-based ILs bearing, for example, [Br]⁻ anions with OH functionalities [58], bis-imidazolium bromide functionalized with COOH groups [59], and cellulosic poly(ILs) ([Cellmim][Br]) [60], or polymeric imidazolium-based ILs [61] are also efficient catalysts for CO₂ cycloaddition to epoxides, producing high cyclic carbonate yields, ranging from 92 to 99 %. Despite the high cyclic carbonate yields obtained, the majority of these studies have relied on high reaction temperatures (up to 130 °C) to enhance the selectivity towards cyclic carbonates [60–62], and long reaction times (4 - 48 h) [55,58,61]. The reaction conditions in these approaches lead to high energy consumption and reduced sustainability for the cyclic carbonate synthesis. Thus, few attempts have been made to employ low-reaction temperature and reduce the time of the CO₂-epoxy cycloaddition reaction by using non-functionalized imidazolium-based ILs, however, it has been shown that they are more effective combined with a co-catalyst such as ZnCl₂ (yield =95 %, time =1 h, at 100 °C) [63].

Nevertheless, imidazolium ILs bearing halogen anions, such as Cl^- , Br^- , and I^- , have also been used for cyclic carbonate synthesis from CO_2 and monofunctional epoxy resin as a single-component catalyst, yielding 60 to 80 % of cyclic carbonates within a short reaction time (3 to 6 h) under mild conditions ($T = 50 - 100\text{ }^\circ\text{C}$) without the use of a solvent or a co-catalyst [46,54,64,65]. It has been proven that imidazolium cation plays an important role in CO_2 absorption, particularly in the presence of the acidic protons in the imidazolium ring, as they participate in the stabilization of intermediates during the cycloaddition of CO_2 to epoxides, as shown in Fig. 6(B) [46,54]. A typical CO_2 cycloaddition reaction mechanism to epoxide is initiated by imidazolium-based IL via anionic initiation route, as shown in Fig. 6(C).

1.3.3. Effect of ionic liquids on properties of epoxy networks

Epoxy materials exhibit a wide range of T_g (typically from -50 to $180\text{ }^\circ\text{C}$), which can be tuned based on the desired applications. Thus, the incorporation of ILs into epoxy systems such as 1-ethyl-3-methylimidazolium dicyanamide [66], *N, N'*-dioctadecylimidazolium iodide [67], 1-(3-aminopropyl)-3-butylimidazolium bis(trifluoromethylsulfonyl)imide, and tetrabutylammonium leucine [68], enhanced the performance characteristics of epoxy systems, resulting in elevated T_g values ranging from 187 to $212\text{ }^\circ\text{C}$ [69]. The improved rigidity of epoxy networks can significantly lead to improved flame retardancy. Recent studies have showed that using 30 wt% phosphorous-containing IL with DGEBA epoxy prepolymer have significantly reduced the heat release rate from 1099 kW/m^2 (epoxy/jeffamine) to 300 kW/m^2 [70].

On the other hand, other studies have found that ILs exert a plasticizing effects on epoxy thermosets, for example, phosphonium-based ILs (20 phr) resulted in a significant decrease in T_g of the epoxy-amine networks and storage modulus which can be used for developing flexible conductive electrolytes [71–73]. While, the effect of the amount and type of ILs on the epoxy networks, limited research investigating the effect of the incorporation of metals into ILs. In this context, Soares et al. have studied the magnetic properties of imidazolium and phosphonium-based ILs bearing $[\text{FeCl}_4]$ anions on the epoxy resin which showed microwave absorbing properties [74].

2. Aims of the thesis

The main aim of this thesis is to explore the potential of imidazolium-based ILs as homogeneous catalysts/initiators for epoxy ring opening.

The specific aims of this work were identified:

- To study epoxy–dicarboxylic acid copolymerization catalyzed by ILs, leading to the formation of epoxy networks.
- To investigate epoxy–anhydride copolymerization accelerated by metal-based and metal-free ILs leading to epoxy networks.
- To explore epoxy-CO₂ cycloaddition catalyzed by metal-based and metal-free ILs producing cyclic carbonates, which are potentially applicable for the synthesis of non-isocyanate polyurethanes (NIPUs).

3. Experimental part

This doctoral thesis was conducted in the framework of various and kind cooperation with colleagues from national institutes, Institute of Macromolecular Chemistry CAS (IMC), Institute of Inorganic Chemistry CAS (IIC), University of Chemistry and Technology in Prague (UCT), Faculty of Chemical Technology, Faculty of Chemical Technology of University of Pardubice (UPCE), and international collaborations such as Polymer Materials Engineering at INSA Lyon, and Center for Advanced 2D Materials at the National University of Singapore.

The experimental part of my PhD work includes the use of different types of imidazolium-based ILs (metallic and non-metallic) in epoxy ring-opening polymerization with functional compounds, such as anhydride, dicarboxylic acid, or carbon dioxide (CO₂), as shown in Fig. 7(a). Metal-based ionic liquids (MILs), namely (BMIM)FeCl₄, (BMIM)₂ZnCl₄, and (BMIM)₂CoCl₄ were prepared by Ing. Petra Ecorchard, PhD (from IIC), and Ing. Jan Honzíček, PhD (UPCE), and their structures are depicted in Fig. 7(d). I performed reactions of epoxy–anhydride and epoxy–dicarboxylic acid under conventional heating followed by a curing process in an oven to obtain final crosslinked networks. I also conducted the epoxy-CO₂ cycloaddition experiments during my internship at the IMP laboratory, INSA Lyon, France, which was partially financed by the GAUK grant (project no. 413022). All used reactants, synthesized or commercially purchased and their acronyms are shown in Fig. 7(b-d).

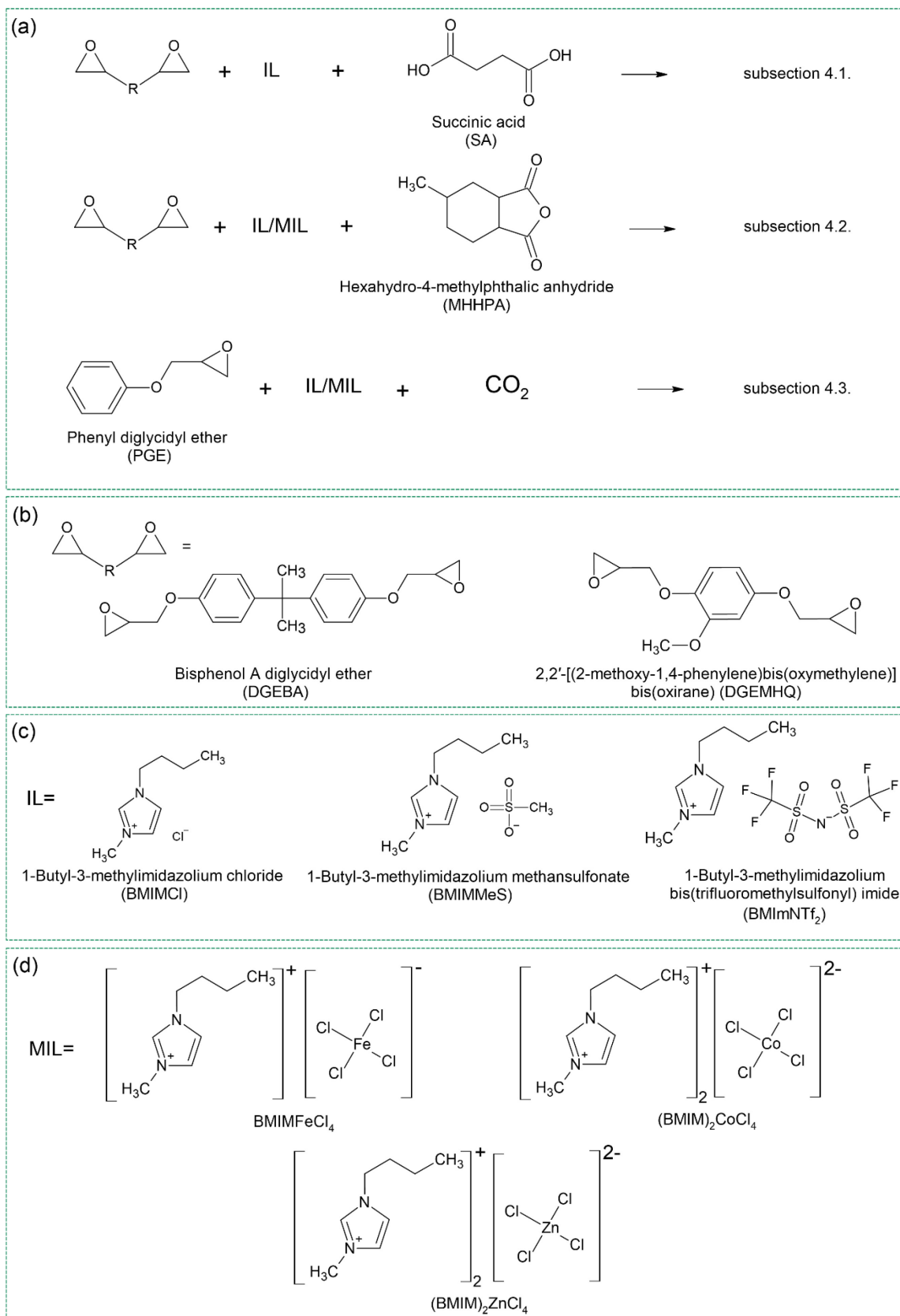


Fig. 7. (a) Schemes of the different epoxy copolymerization reactions performed using IL or MILs, (b) Structures of epoxy resins used (commercially available and synthesized), (c) Structures of commercially purchased ILs and their acronyms, and (d) Structures of MILs and their acronyms.

The epoxy reactions were monitored by key characterization techniques that helped in detecting the complete curing reactions are briefly described below. The data obtained from characterization experiments were conducted in our department at IMC or collaboration with other research institutes:

Fourier-transform infrared spectroscopy (FTIR): characterization of ILs structures, and following the reaction between epoxy and anhydride, CO₂, or dicarboxylic acid. Measurements were conducted at IMC.

Near-infrared spectroscopy (NIR): monitoring of the epoxy/anhydride reactive mixture under non-isothermal mode. Measurements were performed by Ing. Jan Honzíček, PhD (UPCE).

Differential scanning calorimetry (DSC): conducting reactive mixtures of epoxy–anhydride to detect the catalytic reactivities of MILs. Measurements were conducted at IMC.

Nuclear Magnetic Resonance (NMR): the final polymerization products and intermediates were measured, determined, and analyzed by MSc. Andrii Mahun (IMC).

Matrix-assisted laser desorption/ionization-time of flight mass spectroscopy (MALDI-TOF): the process of polymerizations, analysis of end groups, presence of intermediates formed with ILs, and detection of initiation species. Measurements were performed by Ing. Zuzana Walterová (IMC).

Density Functional Theory (DFT): detection of the mechanism of the CO₂ – epoxy cycloaddition reaction using imidazolium-based IL using DFT calculations and solvation models. Measurements and analyses were conducted by Ing. Ctirad Červinka, Ph.D (UCT).

Thermogravimetric analysis (TGA): decomposition temperature of ILs, epoxy networks, the thermal stability of networks, char yields, and water content in MILs. All TGA experiments were carried out at IMC.

Dynamic mechanical thermal analysis (DMTA): measurement of shear deformation, and the main transition temperature (T_g), which was detected as the maximum of the $\tan \delta$ peak. DMTA experiments were performed by Ing. Jiří Hodan (IMC).

Further information on particular instruments, equipment, and experimental conditions can be found in the detailed description in the publications used to describe this thesis (appendices to this thesis).

4. Results and discussion

4.1. Epoxy-dicarboxylic acid copolymerization reaction

Appendix 1: VOC-free tricomponent reaction platform for epoxy network formation mediated by a recyclable ionic liquid

4.1.1. Catalytic properties of ionic liquid in epoxy-dicarboxylic acid copolymerization

Herein, the reactions of bisphenol A diglycidyl ether (DGEBA) and succinic acid (SA) in the presence of 1-butyl-3-methylimidazolium-based ILs (BMIMCl, BMIMeS, and BMIMNTf₂) (see structures in section 3., Fig. 7(a-c)). Initially, the two-component systems DGEBA/SA without IL and DGEBA/BMIMCl without SA were subjected to mixing under heating at 80 °C for 24 h, and the reaction progress was followed by FTIR to investigate the specific roles of dicarboxylic acid and IL in the epoxy polymerization process (Fig. 8).

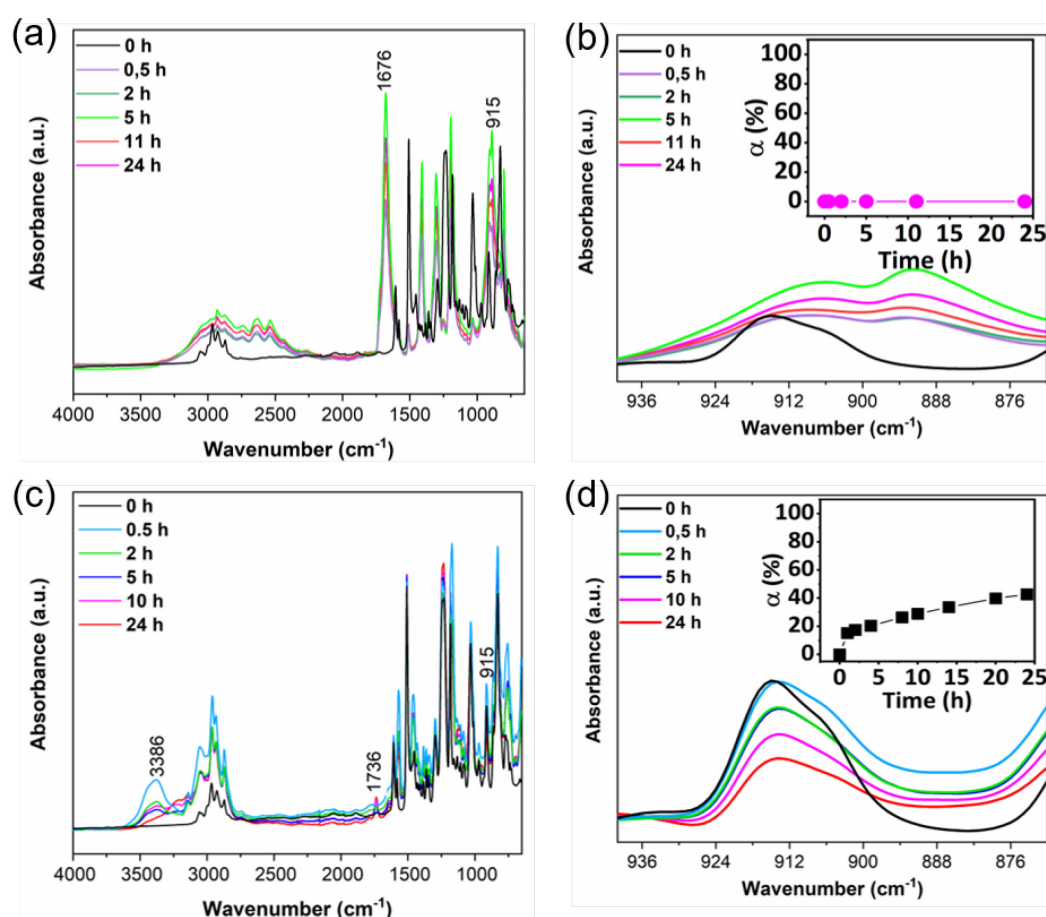


Fig. 8. FTIR spectra and zoomed FTIR spectra of the band at 915 cm⁻¹ with the conversion (α (%)) curves versus time as insets, respectively for the bicomponent systems: (a,b) DGEBA/SA, and (c,d) DGEBA/BMIMCl. Reproduced from [75].

The analysis of the FTIR spectra of the DGEBA/SA system revealed the persistence of the epoxy band (at 915 cm^{-1}) even after heating for 24 h at $80\text{ }^{\circ}\text{C}$ (Fig. 8(a,b)). This observation indicates that SA alone is not sufficient to undergo a reaction with DGEBA under these conditions in the absence of a catalyst. These results are consistent with the existing literature, suggesting that the epoxy/acid reaction is primarily triggered by amines, imidazole, pyridine derivatives, or organic catalysts at low temperatures. The DGEBA/BMIMCl system underwent a color change from transparent yellow to dark red at $80\text{ }^{\circ}\text{C}$, indicating an increase in aromaticity and molecular weight. The consumption of epoxy groups is verified by FTIR for this system, but the rate of epoxy conversion is notably slow, reaching only 50% after 24 h (Fig. 8(c,d)).

The three-component system DGEBA/SA/BMIMNTf₂ did not demonstrate epoxy consumption in the FTIR spectra due to the poor nucleophilicity and miscibility of the BMIMNTf₂ in the reaction mixture between DGEBA and SA (Fig. 9(a,b)). On the other hand, the DGEBA/SA/BMIMMeS system revealed a homogeneous mixture with proven epoxy ring opening by following the decrease in the band at 915 cm^{-1} and the appearance of the ester group at 1730 cm^{-1} , as seen in the FTIR spectra (Fig. 9(c)). However, this system showed slow epoxy conversion as full consumption was obtained after approximately 10 h of reaction (Fig. 9(d)). The DGEBA/SA system containing BMIMCl showed the highest epoxy conversion rate within 5 h of the reaction, as evidenced by the complete absence of the epoxy band at 915 cm^{-1} and the formation of ester functions at 1730 cm^{-1} (Fig. 9(e,f)).

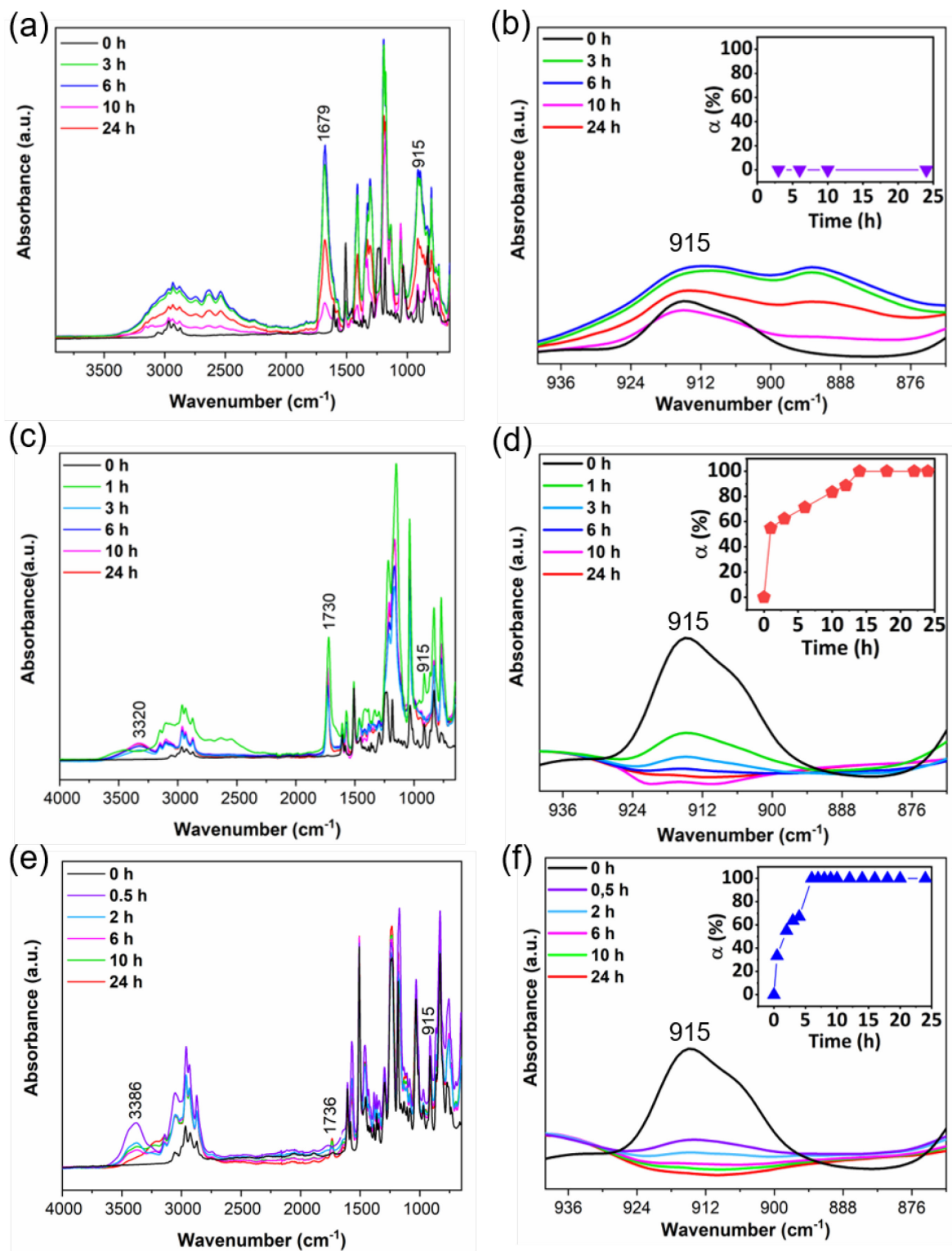


Fig. 9. FTIR spectra and zoomed FTIR spectra of the band at 915 cm^{-1} with the conversion (α (%)) curves versus time as insets, respectively for the tricomponent systems: (a,b) DGEBA/SA/BMIMNTf₂, (c,d) DGEBA/SA/BMIMeS and (e,f) DGEBA/SA/BMIMCl. Reproduced from [75].

Furthermore, the ^1H NMR spectra confirmed FTIR results by showing a progressive reduction in the signal intensity corresponding to the epoxy rings (signal 1 at 2.68 ppm, 2.82 ppm and signal 2 at 3.29 ppm, Fig. 10(a)), together with the appearance of new signals related to the dicarboxylic acid functions (signals 16 and 16', Fig. 10(a)), proving the reaction between DGEBA and SA. This indicates the triple role played by BMIMCl as *i*) an initiator of the reaction between DGEBA and SA, *ii*) a solvent for SA, and *iii*) a compatibilizing agent in the DGEBA/SA reaction.

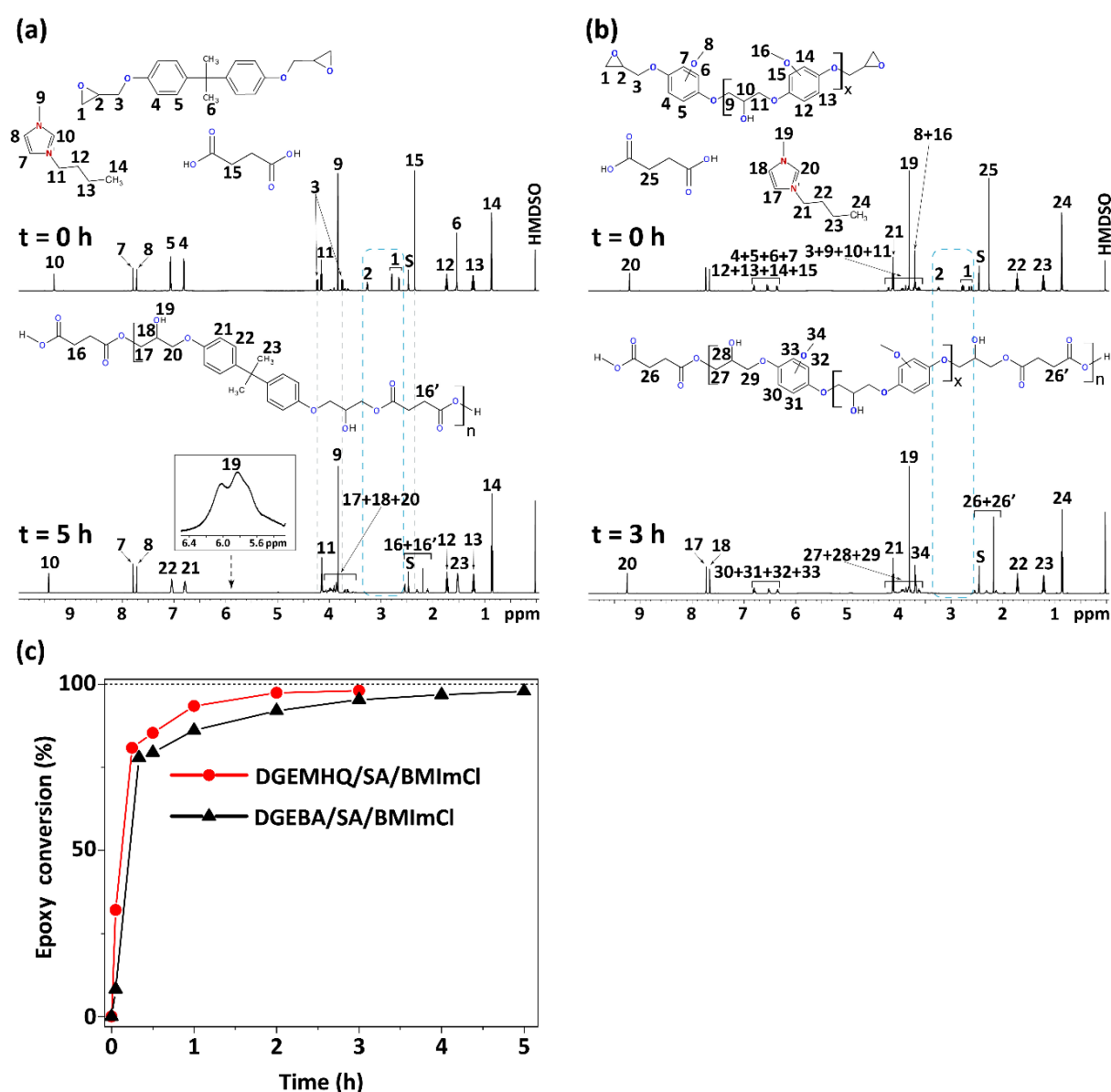


Fig. 10. ^1H NMR spectra of (a) DGEBA/SA/BMIMCl measured at $t=0$ h and after 5 h (full epoxy consumption), and (b) DGEMHQ/SA/BMIMCl measured at $t=0$ h and after 3 h (full epoxy consumption), and (c) Epoxy conversion curves over time calculated from ^1H NMR data for DGEBA/SA/BMIMCl and DGEMHQ/SA/BMIMCl systems. Reproduced from [75].

After the results obtained with the petroleum-based epoxy (DGEBA), a bio-sourced epoxy monomer based on vanillin, 2,2'-[(2-methoxy-1,4-phenylene)bis(oxymethylene)]bis(oxirane), was synthesized (details are given in Appendix 1) and applied to the epoxy-SA coupling reaction. The vanillin-based epoxy was synthesized by functionalizing methoxyhydroquinone with epichlorohydrin to obtain an epoxy monomer bearing two oxirane rings (DGEMHQ) (see the structure in section 3., Fig. 7(b)). Subsequently, this epoxy monomer is considered a suitable bio-based alternative to DGEBA as it contains aromatic rings, which are essential for the formation of epoxy networks exhibiting high thermal and mechanical properties.

Accordingly, the DGEMHQ/SA reaction proceeded in the presence of BMIMCl under the same conditions as for DGEBA (mixing at 80 °C, 24 h) and was followed by ¹H NMR spectroscopy, which indicated the ring-opening of epoxy groups in DGEMHQ, by the disappearance of the corresponding signal 1 (at 2.68 ppm and 2.82 ppm) and signal 2 (at 3.29 ppm) after 3 h of reaction (Fig. 10(b)). The DGEMHQ epoxy conversion versus time was further compared with that of DGEBA based on ¹H NMR analysis and was found to be completed within 3 h of reaction, faster than the DGEBA/SA/BMIMCl system (Fig. 10(c)).

In conclusion, it appears that the bio-based epoxy DGEMHQ exhibits a high reactivity towards dicarboxylic acid using BMIMCl at low temperatures. This highlights the sustainable reaction conditions and suggests the potential substitution of petroleum-derived epoxy resins with bio-based ones.

4.1.2. Proposed mechanism of epoxy-acid ring-opening polymerization mediated by imidazolium-based ionic liquid

To provide a well-established initiation reaction mechanism by BMIMCl, the final product of the DGEBA/SA/BMIMCl system obtained after 24 h was measured by MALDI-TOF, which allowed a comprehensive study of the chemical changes and reactions occurring during the reaction. Analysis of the MALDI-TOF mass spectrum revealed three mass distributions with an increment of 458 Da attributed to the repeating unit of DGEBA-SA (Fig. 11(a,b)). The different positions of the signals revealed different end groups of the DGEBA-SA unit, including COOH, and chloride (Fig. 11(b)). Thus, the analysis of these end groups enabled the investigation of the epoxy-acid ring-opening initiation mechanism via IL. The possible IL-based initiation routes of epoxy ring-opening have been properly described in the literature as it was mentioned earlier in subsection 1.3.1 (Fig. 5). Since there was no evidence of formed intermediates containing imidazolium cation, such as deprotonated or dealkylated

imidazolium-ring, based on both ^1H NMR and MALDI-TOF, we speculated that the initiation of epoxy ring opening involves the anionic species of the IL (chloride anion). Based on these results, we proposed an initiation mechanism of the DGEBA/SA/BMIMCl system involving the nucleophilic attack of the chloride anion of the IL (Fig. 11(c)).

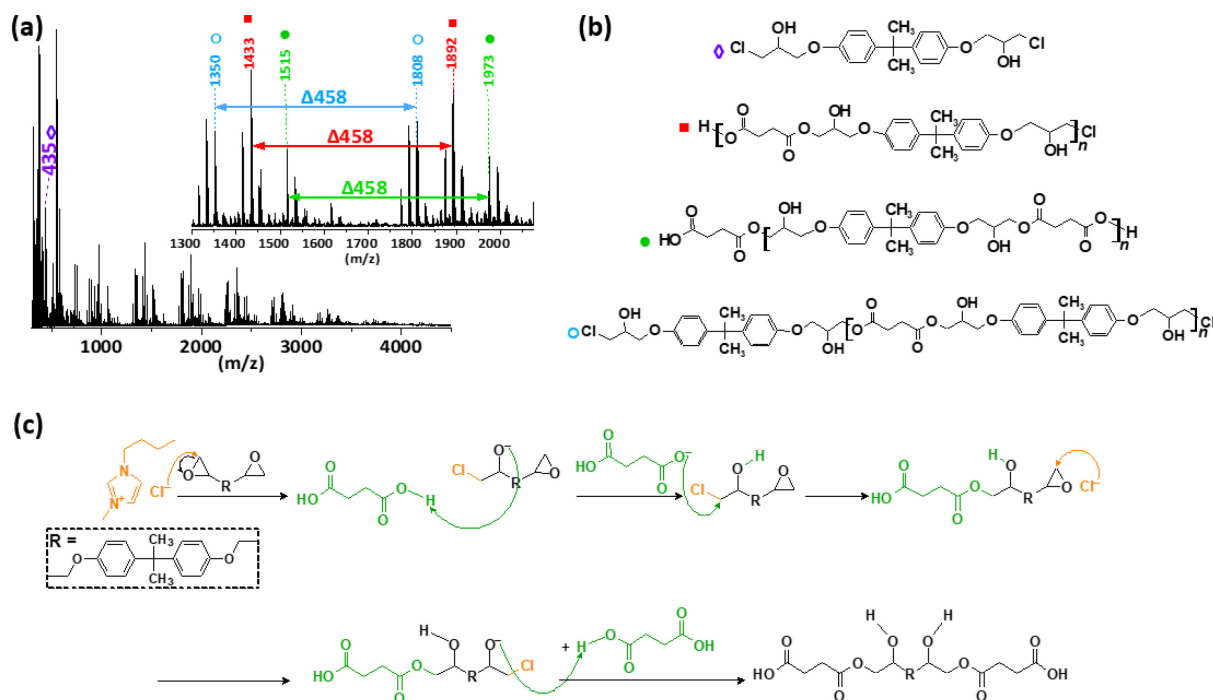


Fig. 11. (a) MALDI-TOF mass spectra of the system DGEBA/SA/BMIMCl after 24 h showcasing the three main mass distributions (b) the different structures and intermediates detected based on MALDI-TOF mass spectra with their corresponding symbols, and (c) suggested initiation mechanism for DGEBA/SA/BMIMCl through BMIMCl-triggered acid-epoxy addition. Reproduced from [75].

In the first step, the Cl^- anion acts as a Nu^- and attacks the oxirane ring at the least hindered carbon. Meanwhile, the acidic proton of SA activates the oxirane ring. Subsequently, the oxirane ring opens and terminates by chloride, followed by nucleophilic attack of the carboxylate anion of SA on the epoxy carbon associated with chloride, releasing Cl^- , which becomes available for the second initiation of the epoxy ring opening (Fig. 11(c)). This results in an alternating linear epoxy-acid structure, as shown in the MALDI-TOF spectrum by the green circle-marked structure (Fig. 11(b)). The proposed initiation mechanism provides evidence that SA serves as a building block for the epoxy-acid copolymer and BMIMCl acts as a catalyst/initiator of the coupling reaction between DGEBA and SA.

4.1.3. Thermomechanical properties of the cured epoxy-dicarboxylic acid networks

To obtain a fully crosslinked epoxy network, the epoxy-acid reaction must undergo post-curing at high temperatures, and the amount of IL must be minimized to allow the reaction between the epoxy and SA without compromising the final thermal and mechanical properties. The optimization allowed a molar ratio of (1/1/0.2) for the DGEBA/SA/BMIMCl and DGEMHQ/SA/BMIMCl systems, which followed a post-curing process for 48 h at 120 °C, and analysis of the thermal and mechanical properties using TGA and DMTA methods (Table 1).

Table 1. DMTA and TGA analysis results of post-cured systems.

System	DMTA results	TGA results	
	$T_{\alpha, \text{DMTA}}, ^\circ\text{C}$	$T_{d5\%}, ^\circ\text{C}$	Char yield at 790 °C, wt%
DGEBA/SA/BMIMCl	57	331	9
DGEMHQ/SA/BMIMCl	55	324	25

Both bio- (DGEMHQ/SA/BMIMCl) and petroleum-based (DGEBA/SA/BMIMCl) materials exhibited the characteristic storage modulus (G') curve shape of thermosets, as evidenced by the rubbery plateau that gradually increases with the temperature, unveiling the formation of a covalent network (Fig. 12(a)).

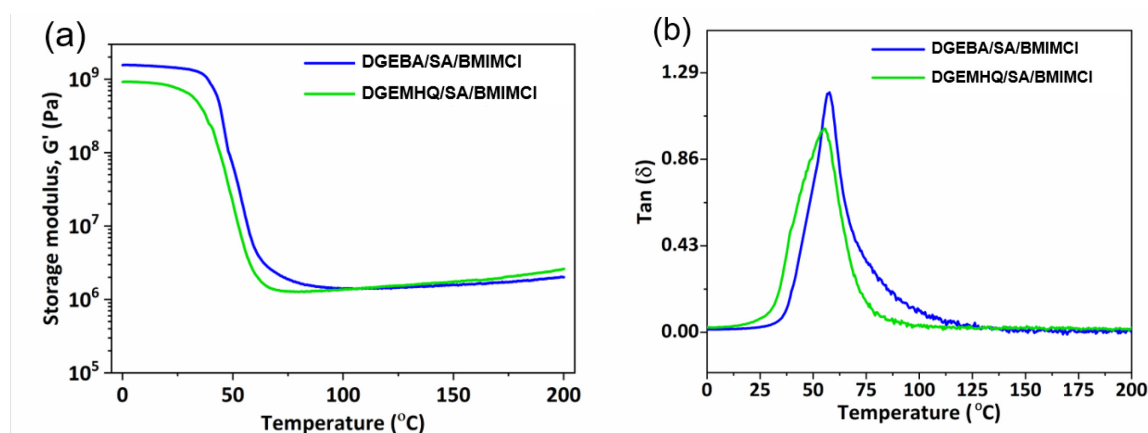


Fig. 12. (a) DMTA analysis showing G' versus temperature curves and (b) $\tan(\delta)$ versus temperature showing the glass transition curves, where the maximum of this curve is the glass transition temperature value (T_{α}). Reproduced from [75].

The secondary hydroxyl groups generated during the epoxy-acid coupling reaction allowed further crosslinking as they can *i)* react with SA groups through condensation to form ester linkages, *ii)* interact with epoxy to facilitate ring opening and form ether linkages, or *iii)*

undergo transesterification with ester bonds. The DMTA results also showed a similar T_{α} , which is related to the glass transition temperature taken at the maximum of the peak from the curve $\tan(\delta)$ vs. temperature (Fig. 12(b)) for both DGEBA/SA/BMIMCl and DGEMHQ/SA/BMIMCl with values of 57 and 55 °C, respectively (Table 1). Furthermore, the DGEBA/SA/BMIMCl and DGEMHQ/SA/BMIMCl systems were found to have a high thermal stability as evidenced by the high $T_{d5\%}$ (up to 330 °C, Table 1). Subsequently, the final cured epoxies (DGEBA and DGEMHQ) with SA using imidazolium-based IL resulted in solid homogeneous materials. Most importantly, the bio-sourced DGEMHQ/SA/BMIMCl final material could serve as a sustainable alternative for petroleum-based materials in terms of rigidity and mechanical and thermal properties.

4.2. Epoxy-anhydride copolymerization reaction

Appendix 2: Accelerating effect of metal ionic liquids for epoxy-anhydride copolymerization

4.2.1. Catalytic activity of metal-based ionic liquids in the epoxy-anhydride copolymerization

First the DGEBA/MHHPA reactions in the presence of MILs, BMIMCl and the conventional catalyst (1-methylimidazole, 1MIM) (see structures in section 3., Fig. 7(a-d)) was studied using the non-isothermal DSC (Fig. 13).

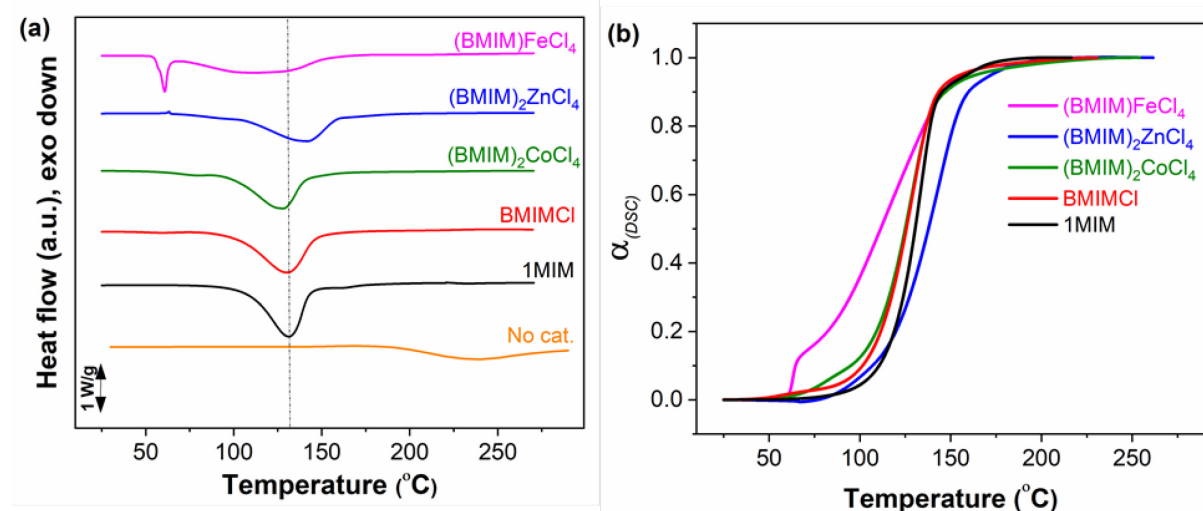


Fig. 13. (a) Dynamic DSC profiles under non-isothermal conditions and (b) DSC conversion (α_{DSC}) curves of the DGEBA/MHHPA non-isothermal crosslinking reaction using 2.70 mol% of catalyst 1-methylimidazole (1MIM), BMIMCl, $(\text{BMIM})_2\text{CoCl}_4$, $(\text{BMIM})_2\text{ZnCl}_4$, or BMIMFeCl_4 at a heating rate of 5 °C/min. Reproduced from [76].

The reactive mixture DGEBA/MHHPA without any catalyst revealed a negligible exothermic peak at a very high temperature (approximately above 230 °C) related to the non-

catalytic curing between epoxy and anhydride (Fig. 13(a)). On the other hand, the reactive mixture of DGEBA/MHHPA using 2.70 mol% of catalyst showed a significant exothermic peak at lower onset temperatures (T_{onset}) than the non-catalyzed mixture, demonstrating the ability of MILs, BMIMCl and 1-methylimidazole (1MIM) to catalyze the reaction and to reach a full conversion of epoxy monomers (Fig. 13(b)). The T_{onset} values of the DGEBA/MHHPA mixtures with MILs were lower (between 57 and 99 °C) than those with BMIMCl and 1MIM, along with a slight decrease in the total reaction heat ($\Delta H_{r,\text{total}}$) (Table 2). Therefore, MILs proved to be efficient catalysts for DGEBA/MHHPA copolymerization, providing fully cured materials with elevated T_g (Table 2, entries (3-5)).

Table 2. Dynamic DSC results of DGEBA/MHHPA (1/1) formulations using 2.7 mol% of catalyst, at a heating rate of 5 °C/min. T_g^a of the cured systems was determined from the second heating run (up to 300 °C at 10 °C/min). Reproduced from [76].

Entry	Formulation	T_{onset} , °C	T_{max} , °C	$\Delta H_{r,\text{total}}$, J/g	T_g^a , °C
1	No cat.	192	237	192±12	110
2	DGEBA/MHHPA/1MIM	106	130	357±21	134
3	DGEBA/MHHPA/BMIMCl	101	131	334±16	128
4	DGEBA/MHHPA/ BMIMFeCl ₄	57	61	343±19	96
5	DGEBA/MHHPA/ (BMIM) ₂ CoCl ₄	97	128	327±14	147
6	DGEBA/MHHPA/ (BMIM) ₂ ZnCl ₄	99	142	331±20	148

The sudden jump in conversion at the low exotherm temperature for the DGEBA/MHHPA formulation with MILs, specifically (BMIM)FeCl₄, led to a different conversion curve shape than that of the reference system with 1MIM and BMIMCl (Fig. 13(b)). To explore the origin of this low-T phenomenon, the DGEBA/MHHPA reactive mixtures with MILs, BMIMCl, or 1MIM, were measured by near-infrared (NIR) spectroscopy measurements in the non-isothermal mode (at a heating rate of 5 °C/min) (Fig. 14). Accordingly, NIR spectroscopy allowed the monitoring of the progress of functional groups initially present or formed during the non-isothermal crosslinking process, including epoxy (4530 cm⁻¹), anhydride (4828 cm⁻¹), ester (5158 cm⁻¹), hydroxyl (the broad overlapping OH bands of alcohol and carboxylic acid functionalities in the region of 6800 – 7130 cm⁻¹) groups and moisture (5252 cm⁻¹) (Fig. 14). All the studied formulations showed a decrease in epoxy and anhydride groups with increasing temperature, along with a gradual increase in ester groups (Fig. 14(a-e)). In contrast, the NIR plots showed that, in all systems, the anhydride group was consumed

faster in the early stage of the reaction and was synchronized with the decrease in moisture. This indicates that the anhydride compound (MHHPA) was hydrolyzed by water at the beginning of the reaction due to the presence of moisture in the formulation resulting from the hygroscopic nature of the MILs. It was revealed that in the MIL-containing systems, the moisture decrease was followed by an increase in the hydroxyl group, which was formed at temperatures of 90, 110 and 60 °C, for the DGEBA/MHHPA systems using $(\text{BMIM})_2\text{CoCl}_4$, $(\text{BMIM})_2\text{ZnCl}_4$, and BMIMFeCl_4 , respectively (Fig. 14(a-c)).

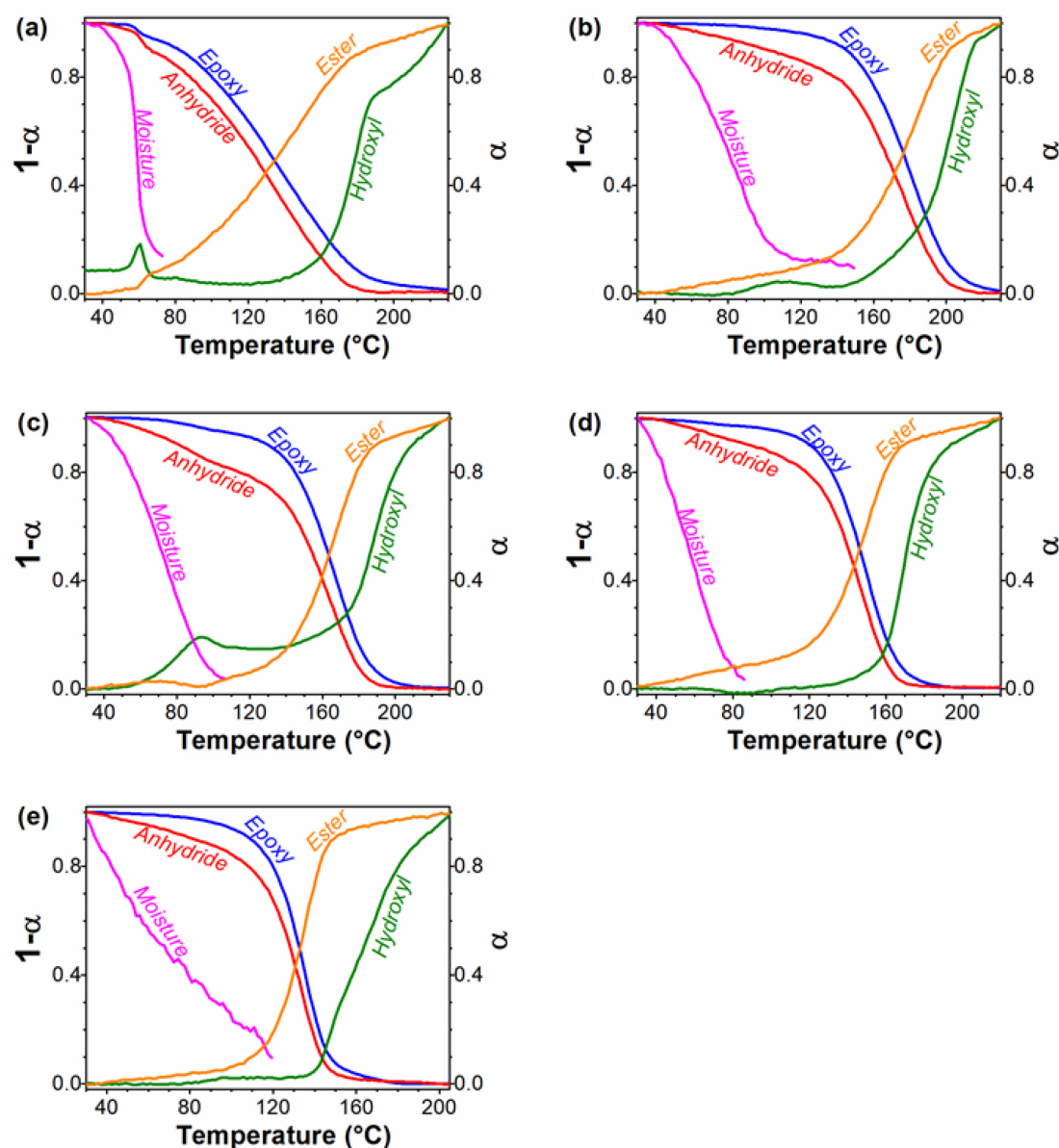


Fig. 14. Non-isothermal NIR spectroscopy (5 °C/min) showing the progress of functional groups in the reactive DGEBA/MHHPA mixtures using: (a) BMIMFeCl_4 , (b) $(\text{BMIM})_2\text{ZnCl}_4$, (c) $(\text{BMIM})_2\text{CoCl}_4$, (d) BMIMCl , and (e) 1MIM . Left Y-axis for epoxy, anhydride and moisture; Right Y-axis for ester and hydroxyl. Reproduced from [76].

This explains that the origin of the low-T exotherm at 60 °C for the DGEBA/MHHPA/BMIMFeCl₄ system is related to the rapid hydrolysis of MHHPA by traces of water initially present in the MILs (Fig. 13(a) and Fig. 14(a)). This hydrolysis process resulted in an increase in the number of acidic groups (COOH), which reacted rapidly with the epoxy groups to form ether linkages. At high temperatures (above 150 °C), all epoxy and acid groups reacted, indicating that a complete curing reaction reached the plateau at the conversion curves (Fig. 13(b)).

4.2.2. Mechanism investigation of the epoxy-anhydride copolymerization

To determine the IL-initiated mechanism of DGEBA/MHHPA copolymerization, MALDI-TOF mass spectrometry was performed. The primary focus was on the initial stage of the reaction to gain an understanding of the first step of initiation. A sample was extracted for MALDI-TOF measurements after a 15 min duration. However, the copolymerization reaction between DGEBA and MHHPA using ILs led to the fast formation of an insoluble fraction due to the rapid curing reaction, making it inappropriate for MALDI-TOF analysis. Therefore, a model reaction between a monofunctional epoxy monomer PGE (see structure in section 3., Fig. 7(a)) and MHHPA was performed in the presence of 1MIM, BMIMCl, or MILs (at 2.70 mol%) at 80 °C for 15 min. The resulting product was fully soluble and thus suitable for MALDI-TOF analysis. First, the reaction PGE/MHHPA/1MIM was performed showing a predominantly singular distribution (with a 318 Da increment). This distribution comprised an alternating MHHPA unit of 168 Da and a PGE unit of 150 Da, terminated with an 82 Da unit corresponding to the 1-methylimidazolium compound (Fig. 15(a)). The detection of this terminal group proved the initiation step that involved the nucleophilic attack of 1MIM on the epoxy ring of PGE, forming an alkoxide (Fig. 15(b)). Subsequently, the alkoxide attacked the anhydride compound, producing a carboxylate anion that can open another epoxy ring, forming an alternating linear copolymer (Fig. 15(b)).

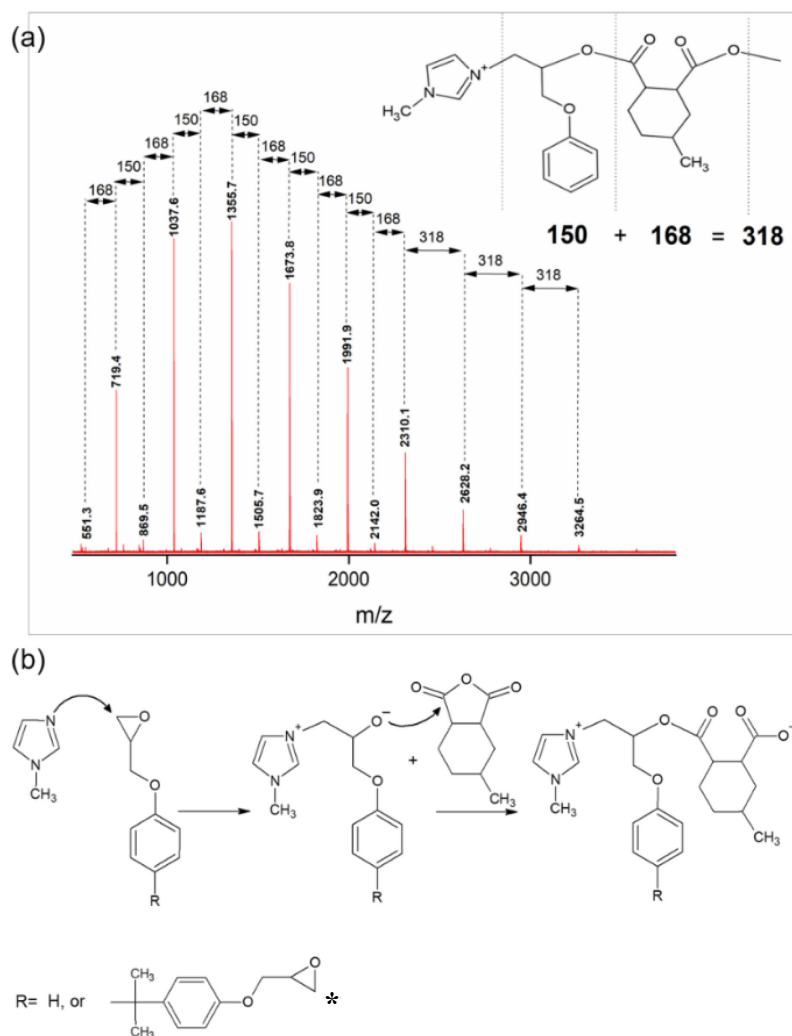


Fig. 15. (a) MALDI-TOF spectrum of reaction PGE/MHHPA/1MIM after 15 min at 80 °C, (b) Proposed initiation and propagation steps for the PGE/MHHPA/1MIM system described as anionic copolymerization via nucleophilic attack of 1MIM. *The mechanism can be adapted also for the bifunctional DGEBA monomer. Reproduced from [76].

The MALDI-TOF spectra of the PGE/MHHPA reaction systems containing MILs indicated five distinct mass distributions, proving the presence of different end groups with the same repeating unit PGE/MHHPA (150+168=318 Da), confirming alternating copolymerization (Fig. 16(a-c)). Thus, the detection of various end groups indicated several initiation mechanisms. The structures marked in black and green (Fig. 16(d)) demonstrate that PGE/MHHPA is end-capped with a dealkylated imidazolium ring (black structure: dealkylation of butyl, and green structure: dealkylation of methyl). This confirms the ‘imidazole’ initiation route of MILs, where the nitrogen atom of the dealkylated imidazolium ring prompted the epoxy ring opening, similar to the 1MIM initiation mechanism (Fig. 15(b)).

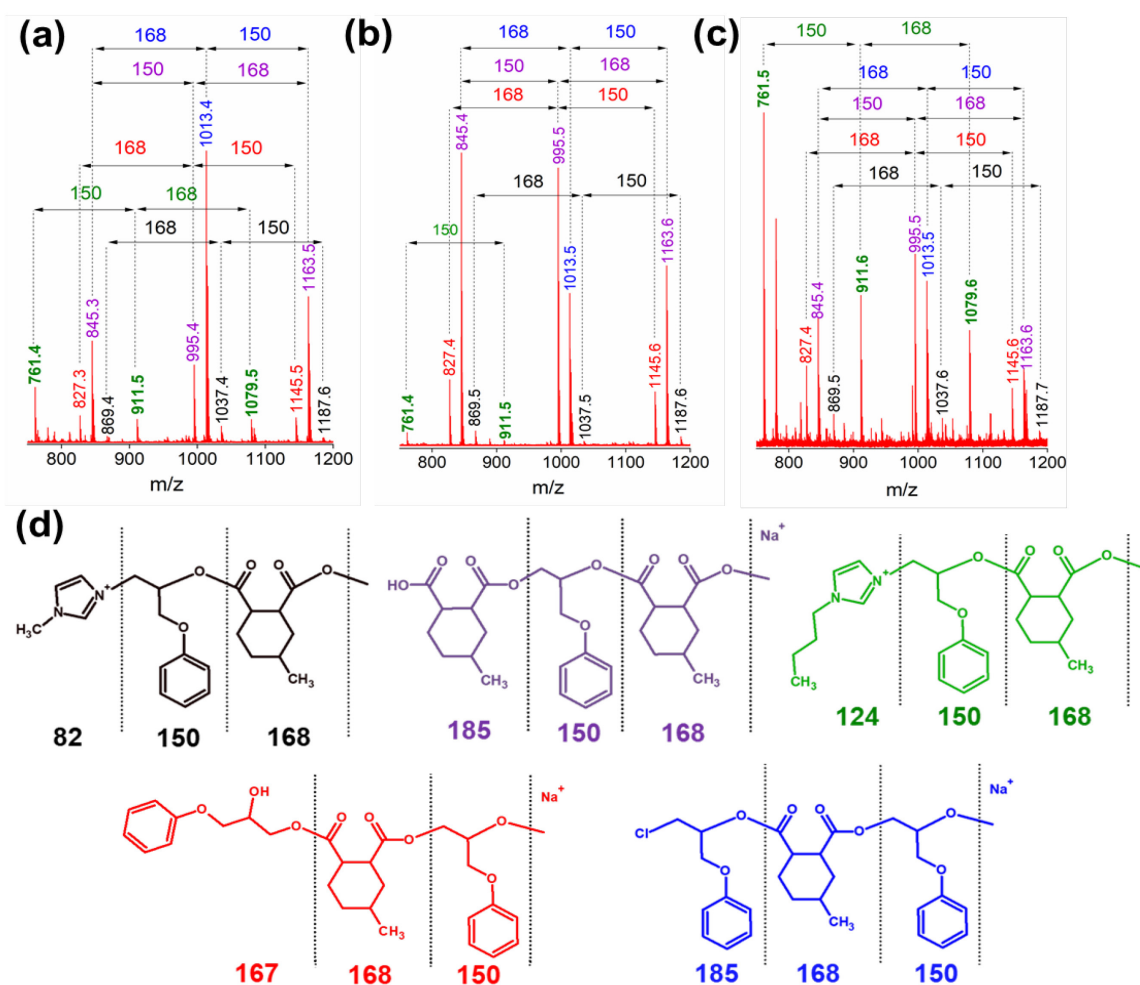
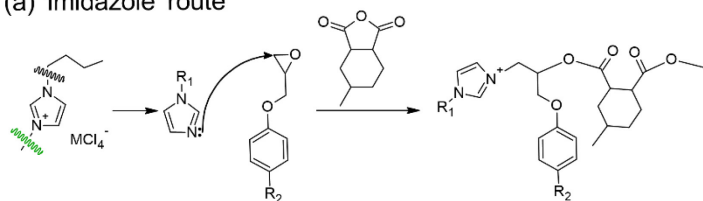


Fig. 16. (a-c) MALDI-TOF mass spectra, and (d) the corresponding detected structures, marked in different colors to represent different end groups, of the reaction mixture of PGE/MHHPA taken after 15 min of reaction at 80 °C catalyzed by (a) BMIMFeCl₄, (b) (BMIM)₂ZnCl₄, and (c) (BMIM)₂CoCl₄. Reproduced from [76].

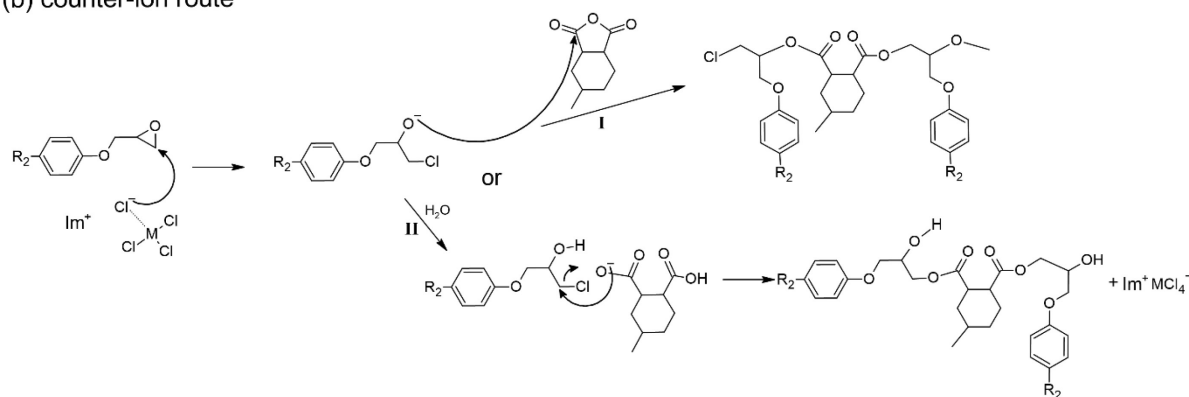
The other three distributions shown in the MALDI-TOF spectra (violet, red, and blue marked structures) were considered to be the dominant distributions for the MIL-catalyzed PGE/MHHPA reaction (Fig. 16(d)). The structures detected with *i*) Cl (blue-marked structure) and *ii*) OH (red-marked structure) as end groups proved an anionic nucleophilic initiation mechanism (Fig. 16(d) and Fig. 17(b)). In this mechanism, the Cl⁻ anion attacks the less sterically hindered carbon of the epoxy ring, generating an alkoxide anion, which can either initiate a direct attack on another anhydride compound, leading to carboxylate anion formation (Fig. 17(b, route I)), or due to its facile hydrolysis, it may initially be converted into a hydroxy-alkoxide, which subsequently reacts with another anhydride group, resulting in carboxylate anion formation (Fig. 17(b, route II)). The reaction in both scenarios proceeded with the

nucleophilic attack of carboxylate anions on another epoxy ring, resulting in the formation of an alternating epoxy-anhydride copolymer (Fig. 16(d), red- and blue-marked structures).

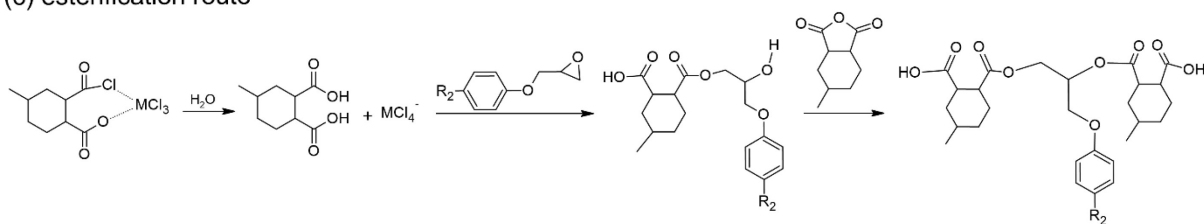
(a) 'imidazole' route

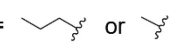


(b) counter-ion route



(c) esterification route



with $M = \text{Fe, Co, or Zn}$ $R_1 =$ 

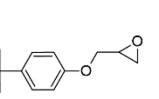
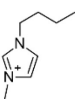
$R_2 =$  or H- $\text{Im}^+ =$ 

Fig. 17. Suggested initiation pathways of epoxy-anhydride reaction initiated by MILs via three different routes: (a) 'imidazole', (b) counter-ion, and (c) esterification route. Reproduced from [76].

The violet-marked distribution of PGE-MHHPA end-capped with the carboxyl group indicated another initiation pathway induced by carboxyl groups formed during the hydrolytic decomposition of anhydride compounds (Fig. 16(d)). As discussed above, these carboxyl groups were formed in the low-T region, which is specific only to epoxy systems containing MILs. We confirm that in this case, the initiation involved the formation of a complex intermediate between the MCl_4 anion and the anhydride ring (Fig. 17(c)). The anhydride- MCl_4 complex formed in the first step allowed the attack of trace amounts of water (likely derived from hygroscopic MILs), resulting in cyclic anhydride hydrolysis and the formation of two

carboxyl groups. The acidic proton of the formed COOH initiated the opening of the oxirane ring, resulting in the formation of hydroxyester group. This initiation pathway, referred to as the ‘esterification pathway’ through the carboxylic acid-epoxy, is usually slow and significant at high temperatures (Fig. 17(c)). In the case of the MIL-catalyzed PGE-MHHPA reaction, the esterification route was fast at a low temperature (80 °C) due to the accelerating effect of MILs. Subsequently, the propagation step involved the additional esterification of hydroxyester groups by their reaction with another anhydride, resulting in the formation of an alternating epoxy-anhydride copolymer with a COOH end-group (Fig. 16(d), structure marked in violet).

In summary, MILs exhibited significant catalytic activities toward the epoxy-anhydride reaction due to the presence of metals (Co, Fe, Zn) in the anionic species. Their presence enhanced the Lewis acidity character of MILs and consequently increased their overall nucleophilicity.

4.2.3. Optimization of the content of metal ionic liquids

ILs are known to exert a plasticizing effect on the final material when used in high quantities, which can reduce the T_g and rigidity of the network. For example, increasing the amount of BMIMFeCl₄ from 0.33 to 2.70 mol% and (BMIM)₂CoCl₄ from 0.05 to 10.00 mol% in the DGEBA/MHHPA reaction resulted in a drastic decrease of the T_g from 148 to 96 °C and 133 to 104 °C, respectively, due to the dilution effect of MILs on the network, resulting in plasticization of the network (Table 3, entries 7-9 and 10-16). Thus, the MIL content in the DGEBA/MHHPA system was optimized to obtain a completely crosslinked material confirmed by maximum values of the reaction enthalpy ΔH_r and T_g (Table 3).

As shown in Table 3, the originally used IL content of 2.70 mol% could be reduced to 0.20, 1.00, and 1.00 mol% of BMIMFeCl₄, (BMIM)₂CoCl₄, and (BMIM)₂ZnCl₄, respectively (Table 3, entries 7, 11, and 18) without reducing T_g and the degree of crosslinking.

Table 3. Dynamic DSC results of the reactive mixture DGEBA/MHHPA using various MIL content for final network optimization, at a heating rate of 5 °C/min. Reproduced from [76].

Entries	DGEBA/MHHPA= 1/1		Dynamic DSC data				
	Catalyst content	Catalyst used	T_{onset} (°C)	T_{max} (°C)	ΔH_r (J/g)	T_g (°C)	
1	-	No cat.	192	237	192	110	
2	2.70 mol%	1MIM	106	130	357	134	
3	2.70 mol%	BMIMCl	101	131	334	128	
4	0.05 mol%	BMIMFeCl ₄	159	207	267	132	
5	0.15 mol%		140	189	342	147	
6	0.20 mol%		132	180	338	148	
7	0.33 mol%		101	167	337	148	
8	0.67 mol%		57	85	331	128	
9	2.70 mol%		57	61	343	96	
10	0.05 mol%		(BMIM) ₂ CoCl ₄	110	137	300	133
11	1.00 mol%			102	137	348	145
12	1.50 mol%	111		142	326	142	
13	2.70 mol%	97		128	327	147	
14	3.50 mol%	92		122	337	130	
15	5.00 mol%	82		112	325	111	
16	10.00 mol%	70		103	216	104	
17	0.50 mol%	(BMIM) ₂ ZnCl ₄	113	146	325	129	
18	1.00 mol%		105	140	347	145	
19	1.50 mol%		104	140	347	144	
20	2.70 mol%		99	142	331	148	

These optimized MIL amounts were significantly lower (by 7-fold for BMIMFeCl₄ and 3-fold for (BMIM)₂CoCl₄ and (BMIM)₂ZnCl₄) compared with the metal-free IL (BMIMCl) and conventional catalyst (1MIM), which is advantageous from an economic and environmental point of view.

4.2.4. Final thermal and mechanical properties of the optimized epoxy-anhydride networks

The DMTA results of the post-cured DGEBA/MHHPA networks showed only a single step change in the storage modulus (G') along with a single peak relaxation $\tan \delta$ at approximately 160 °C (the maximum of this peak is attributed to the T_α value), indicating the formation of homogeneous networks (Table 4, Fig. 18).

Table 4. Results of DMTA and TGA analysis of the DGEBA/MHHPA networks cured using 1MIM, BMIMCl and MILs. Reproduced from [76].

Accelerator			DMTA results			TGA results			
Type	Content		T_{α}	M_c	ν_e	T_{dmax}	T_{d5}	T_{d10}	Char
	mol%	wt%	°C	g/mol	mmol/cm ³	°C	°C	°C	wt.%
1MIM	2.70	1.3	164	490	2.4	437	349	385	7.0
BMIMCl	2.70	2.8	160	435	2.7	427	333	376	8.1
BMIMFeCl ₄	0.20	0.4	171	207	5.6	419	374	393	11.8
(BMIM) ₂ ZnCl ₄	1.00	2.8	167	343	3.4	407	337	359	8.9
(BMIM) ₂ CoCl ₄	1.00	2.8	170	308	3.8	406	356	370	11.4

Nevertheless, the DGEBA/MHHPA systems cured with BMIMCl and (BMIM)₂ZnCl₄ showed an additional small peak on the $\tan \delta$ curve within a sub-glass transition area at approximately 100 °C (Fig. 18(c)). It is suggested that the presence of this peak is due to the partially heterogeneous network structure, which is attributed to the presence of weakly crosslinked local domains. Overall, the MIL-containing networks gave rise to high T_{α} values, between 167 and 170 °C, considerably higher than those obtained with 1MIM and the reference IL (BMIMCl) (Table 4). Additionally, the highly crosslinked networks obtained using MILs were proved by high crosslink density (ν_e) and low molecular weight between crosslinks (M_c) values.

The obtained high ν_e indicated that variations in crosslinking mechanisms occurred during network formation (Table 4). The system DGEBA/MHHPA/BMIMFeCl₄ showed the highest ν_e value, which corresponded well with the DSC results (subsection 4.2.1, Fig. 13) that showed the low-T esterification process, which was significant, especially for this MIL (see subsection 4.2.2, Fig. 17(c)). The TGA results revealed that the networks containing MILs exhibited high thermal stability with a single decomposition step and high T_{d5} and T_{d10} values (Table 4, Fig. 17(b,d)). The highest char yield was obtained for BMIMFeCl₄ and (BMIM)₂CoCl₄-containing systems as a result of network homogeneity and high crosslink density (Table 4). Moreover, the presence of metal anions in the MILs exerted in high char yield due to their high thermal stability.

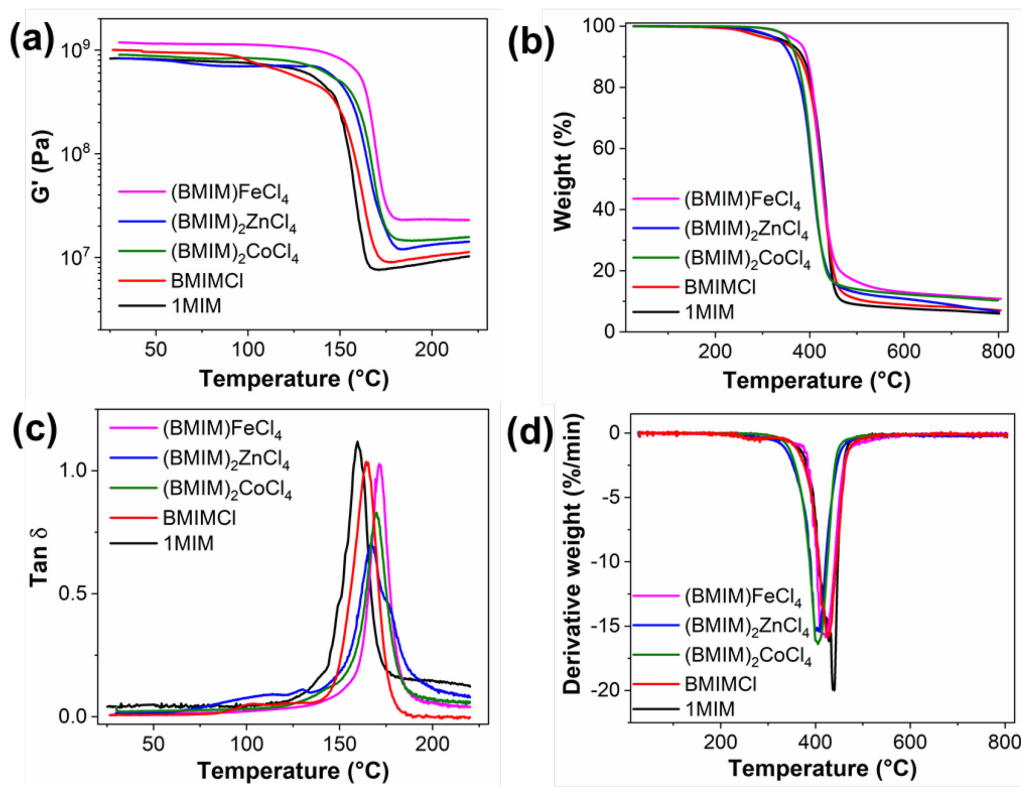


Fig. 18. DMTA and TGA analysis results of DGEBA-MHHPA networks produced using 1MIM, BMIMCl, BMIMFeCl₄, (BMIM)₂ZnCl₄, and (BMIM)₂CoCl₄, by plotting temperature dependence of (a) storage modulus (G') and (c) loss factor ($\tan \delta$), and (b) thermogravimetric and (d) derivative weight curves during TGA under N₂ atmosphere. Reproduced from [76].

4.3. Epoxy-CO₂ cycloaddition reaction

Appendix 3: Fast carbon dioxide-epoxide cycloaddition catalyzed by metal and metal-free ionic liquids for designing non-isocyanate polyurethanes

4.3.1. Catalytic properties of ionic liquids in CO₂-epoxy cycloaddition reaction

Three imidazolium-based ILs, BMIMCl, (BMIM)₂ZnCl₄, and (BMIM)₂CoCl₄ were tested as catalysts for the two-step synthesis of β -hydroxyurethanes under solvent-free conditions (Fig. 19). In the first step, the CO₂ reacts with the epoxy monomer (PGE) bearing one oxirane ring to produce cyclic carbonate (Fig. 19(a), structure 1b). In the next step, the formed cyclic carbonate reacts with *n*-butylamine (BA) to produce β -hydroxyurethanes (Fig. 19(b), structures 1b' and 1b'').

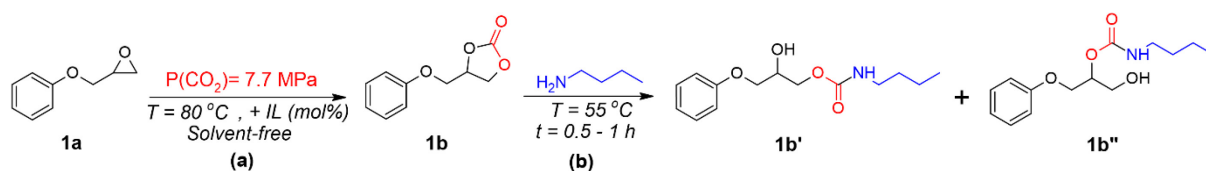


Fig. 19. Simplified schemes of (a) CO₂ cycloaddition reaction for PGE using ILs (BMIMCl, (BMIM)₂ZnCl₄ or (BMIM)₂CoCl₄) and (b) synthesis of β-hydroxyurethanes from cyclic carbonate. Reproduced from [77].

The obtained cyclic carbonates were solids with melting temperatures in the range of 75-88 °C (Table 5). The addition of 10 mol% IL to the PGE monomer under supercritical CO₂ conditions (pressure = 7.7 MPa) at 80 °C for 1 h resulted in a high conversion of epoxy to cyclic carbonates (Table 5).

Table 5. Yields of the cyclic carbonates calculated by FTIR (α_{FTIR}) and NMR (α_{NMR}) spectroscopy from the PGE-CO₂ cycloaddition catalyzed by ILs. Reproduced from [77].

IL	IL loading [mol%]	α_{FTIR} (%)	α_{NMR} (%)	T_m (°C)
BMIMCl	10	94	98	75
(BMIM) ₂ CoCl ₄	10	99	99	88
(BMIM) ₂ ZnCl ₄	10	93	98	76

The structure of cyclic carbonates (Fig. 19, structure 1b) was confirmed by FTIR spectroscopy, which showed the consumption of epoxy bands corresponding to the peak at 915 cm⁻¹, indicating the epoxy ring opening of PGE, and the appearance of a new significant peak at 1787 cm⁻¹, attributed to the C=O carbonyl group in the cyclic carbonate (Fig. 20(a)). Additional FTIR bands have validated the existence of the aromatic backbone of PGE, with bands located at approximately 1600 and 1400 cm⁻¹, and the C-O ether group from the cyclic carbonate was identified by the stretching vibration bands at 1274 and 1037 cm⁻¹ (Fig. 20(a)). FTIR spectroscopy also allowed the calculations of the conversion of epoxy rings, which was 93-99 % (Table 5, α_{FTIR}).

Furthermore, the PGE conversion and the formation of cyclic carbonate structures were confirmed by ¹H NMR spectroscopy (Fig. 20(b,c)). The complete epoxy consumption was evidenced by the disappearance of the corresponding ¹H NMR signals labelled as “a” and “b” at chemical shifts of 2.74 ppm, 2.89 ppm, and 3.34 ppm, respectively (Fig. 20(b,c)).

Additionally, the NMR spectra revealed the appearance of new signals “2” and “3” at 4.38 ppm, 4.62 ppm, and 5.15 ppm, respectively, in the PGE/CO₂ samples with BMIMCl, (BMIM)₂CoCl₄, or (BMIM)₂ZnCl₄, corresponding to the cyclic carbonate rings formation (Fig. 20(b,c)). The yields of cyclic carbonates were also calculated from ¹H NMR and showed high α_{NMR} values of 98 – 99% (Table 5), similar to those of α_{FTIR}.

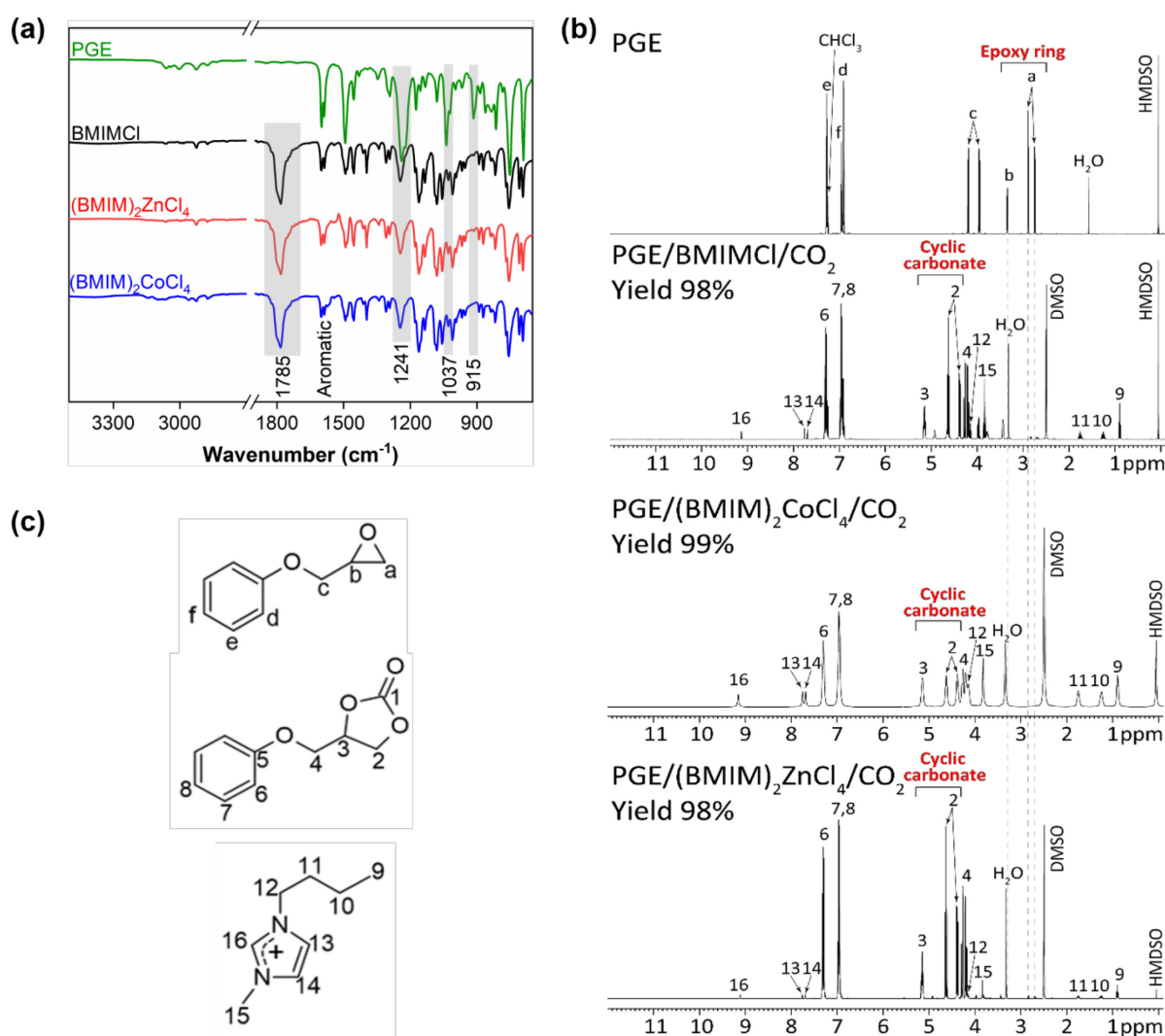


Fig. 20. (a) FTIR and (b) ¹H NMR spectra of the reaction PGE/CO₂/IL products obtained after 1 h and at 10 mol% of BMIMCl, (BMIM)₂CoCl₄, and (BMIM)₂ZnCl₄ and (c) Structures of PGE, cyclic carbonate, and imidazolium ring detected in ¹H NMR spectra. Reproduced from [77].

It is important to mention that these high yields were obtained after a short time (within 1 h) at a low temperature (80 °C) without the addition of any co-catalyst or solvent, demonstrating the high efficiency of the used MILs.

4.3.2. Study of the CO₂-epoxy cycloaddition reaction mechanism initiated by ionic liquid

The reaction mechanism of CO₂ – epoxy cycloaddition initiated by imidazolium-based IL was studied using DFT calculations in combination with ¹H NMR analysis (subsection 4.3.1, Fig. 20). DFT was used to examine all stable transition states and intermediates, and to provide energy barriers for the specific steps of the reaction. First, the energies of reactants, intermediates, products, and transition states were compared by employing various solvation models, including the absence of solvation (Gas), implicit solvation in BMIMCl (Impl.), explicit solvation (Expl.) initiating from reactants solvated by one ion pair (1IP) or two ion pairs (2IP), and complete solvation combining implicit and explicit models (Fig. 21).

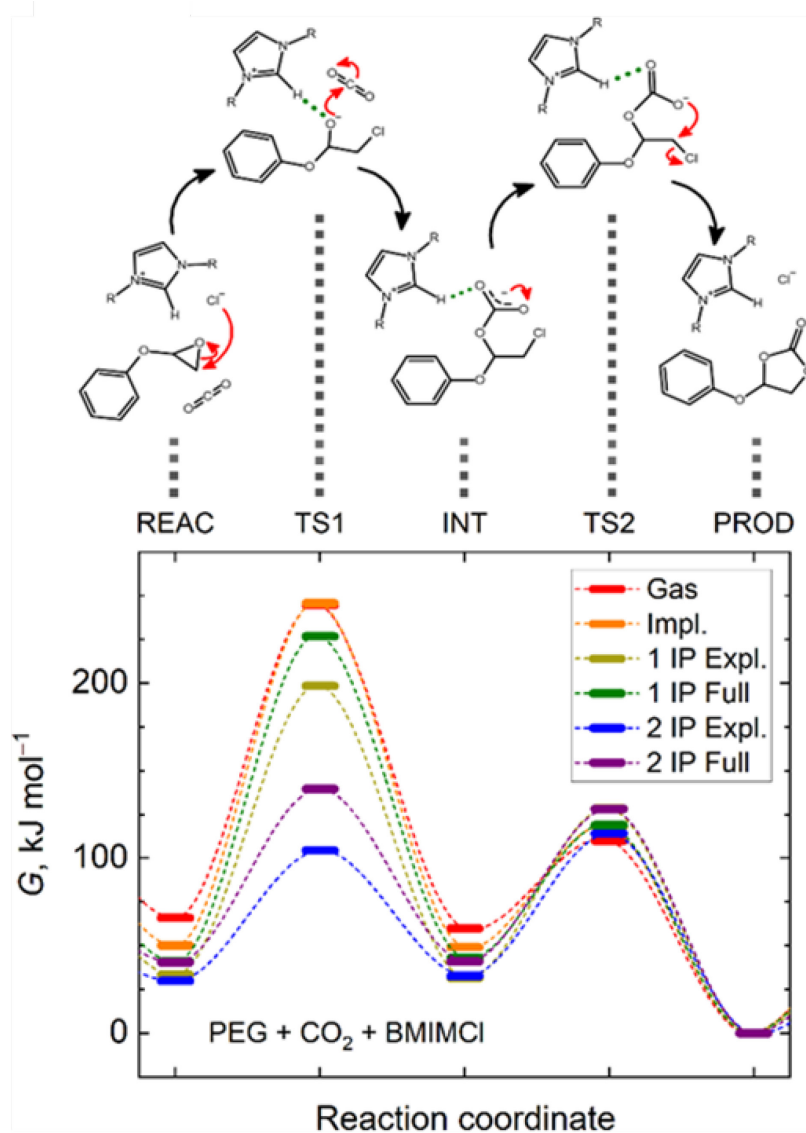


Fig. 21. Gibbs energy profiles during the cycloaddition reaction using the theory level of B3LYP-D3/6-311+G(d,p). Where energies of the reactants (REAC), intermediates (INT), products (PROD), and transition states (TS1 and TS2) are compared. Reproduced from [77].

Accordingly, DFT analysis suggested two transition states (TS1 and TS2) and a stable intermediate (INT) (Fig. 21). The first transition state (TS1) was attributed to the ring opening of PGE after the subsequent nucleophilic attack by the Cl⁻ anion of BMIMCl and the attack of the formed alkoxide on the CO₂ compound (Fig. 21(a), TS1). This led to the identification of the initiation step of the CO₂ – epoxy cycloaddition mechanism using BMIMCl as the ‘counter-ion’ route (see subsection 1.3.2., Fig. 6(B)). In subsection 4.3.1, the ¹H NMR analysis did not show any change in the imidazolium ring, such as the dealkylation of the butyl/methyl chain, confirming the chloride anion initiation route herein proposed (Fig. 21). A stable intermediate structure of chlorinated alcoholate has emerged; however, its optimization to a lower level on the potential energy surface is hindered by the presence of CO₂. The identification of this stable chloro-based intermediate by DFT further demonstrates the involvement of the chloride anion in the reaction.

In addition, DFT calculations predicted the presence of strong hydrogen bonds between the imidazolium ring and the oxygen–anion compounds. This bond plays a significant role in stabilizing the transition states (TS1 and TS2) and lowering the activation energy barrier for the CO₂ cycloaddition (Fig. 21). These results indicate that the imidazolium-based IL acts as a catalyst to promote the conversion of the PGE monomer to cyclic carbonates in a short time.

4.3.3. Synthesis of non-isocyanate polyurethanes from CO₂-epoxy: proof of concept

The monocyclic carbonates, formed by the reaction between PGE and CO₂ using BMIMCl, (BMIM)₂ZnCl₄, and (BMIM)₂CoCl₄, were reacted with BA at 55 °C for 1 h, without the addition of any co-catalyst, to produce a non-isocyanate urethane structure, β-hydroxyurethane (subsection 4.3.1., Fig. 19(b), structures 1b’ and 1b’'), as a proof of concept for the potential synthesis of NIPUs. It is commonly known that the reaction between cyclic carbonates and amines usually requires high temperatures, catalysts and solvents [78]. Herein, cyclic carbonates (subsection 4.3.1., in Fig. 19 structure 1b) were readily mixed with BA at low temperatures, resulting in homogeneous transparent mixtures without the addition of a solvent. The formation of urethane linkages in the formed β-hydroxyurethanes was followed by FTIR spectroscopy (Fig. 22(a-c)). Initially, the cyclic carbonates exhibited a band at 1780 cm⁻¹, which is characteristic of the C=O bond of the cyclic carbonate ring (Fig. 22(a-c)). After the subsequent reaction between the cyclic carbonate and BA, the band at 1780 cm⁻¹ gradually disappeared over time (0.5 h to 1 h), thereby proving the opening of the cyclic carbonate ring. A new peak at approximately 1697 cm⁻¹ was formed and attributed to the urethane C=O bond (Fig. 22(a-c)).

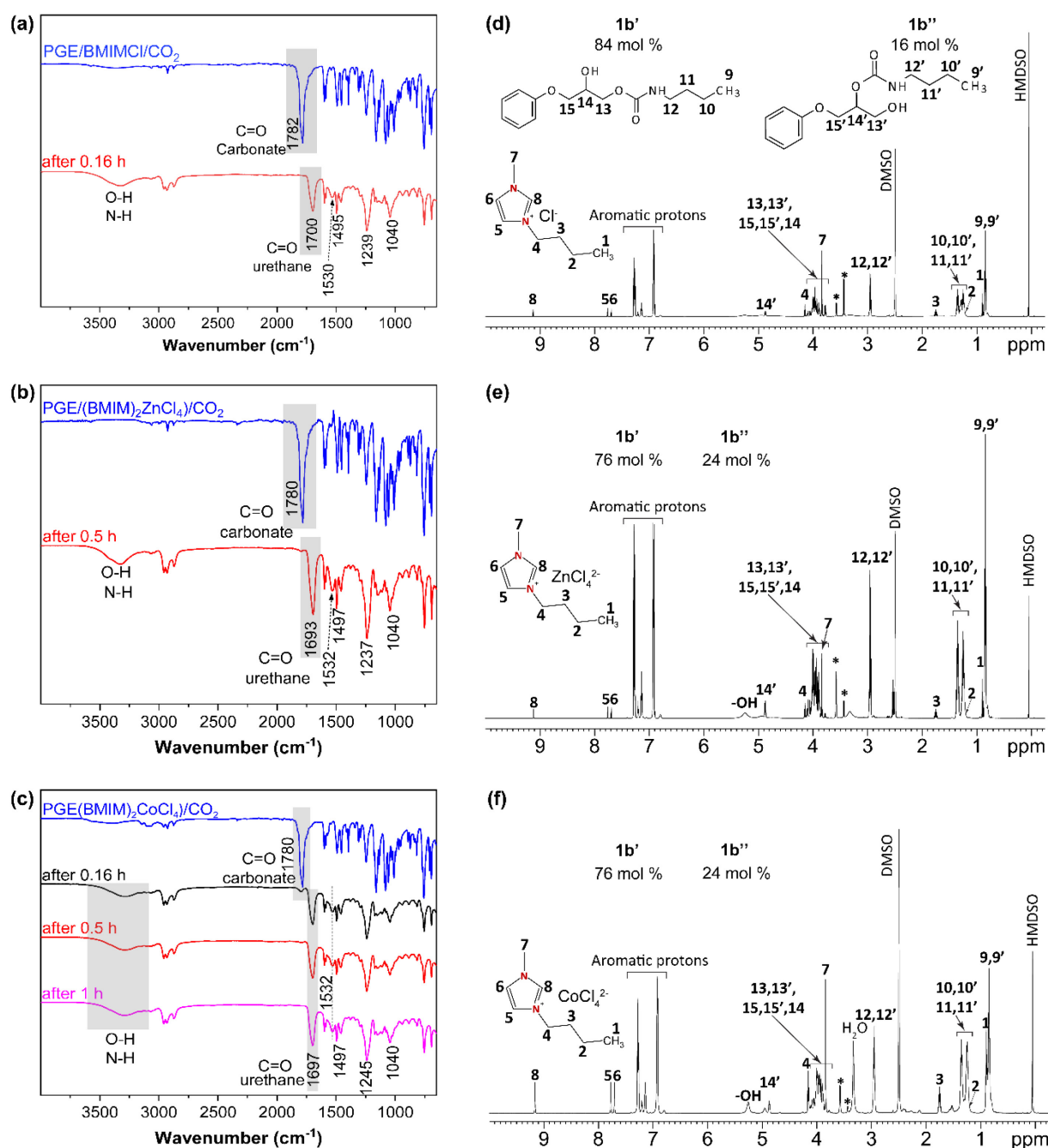


Fig. 22. FTIR and ¹H NMR spectra of the β-hydroxyurethanes resulted from cyclic carbonates containing (a,d) BMIMCl, (b,e) (BMIM)₂ZnCl₄, (c,f) (BMIM)₂CoCl₄. The asterisks (*) represent impurities. Reproduced from [77].

Additionally, the FTIR spectra displayed new bands consistent with the formation of urethane linkages, including bands at 3100 - 3500 cm⁻¹ (O-H and N-H bonds), 1532 cm⁻¹ (N-H in-plane band), 1245 cm⁻¹ (C-N stretching), and 1040 cm⁻¹ (C-O stretching) (Fig. 22(a-c)). These findings were supported by the ¹H NMR analysis, which showed that cyclic carbonates were converted to urethanes, as evidenced by newly formed signals at 12 and 12' (-CH₂-

protons adjacent to $-\text{NH}-(\text{C}=\text{O})-$, Fig. 22(d-f)) and the disappearance of the cyclic carbonate signals initially present at 4.38 ppm, 4.62 ppm, and 5.15 ppm (subsection 4.3.1, Fig. 20(b,c)).

In particular, the NMR analysis identified the structures of the two formed isomers of β -hydroxyurethanes. One isomer contained a secondary hydroxyl, while the other contained a primary hydroxyl, structures 1b'' and 1b'', respectively (Fig. 22(d-f)). Subsequently, the yields of these isomers were found to be dependent on the IL used in the initial reaction. For example, BMIMCl yielded 84% of isomer 1b', while MILs resulted in 76% of the same isomer (Fig. 22(d-f)). Nevertheless, the isomer 1b' represents the majority of the product in all cases, corroborating the results from the literature [79]. Consequently, depending on the IL used in the starting material (cyclic carbonate), it is possible to tune the yield of β -hydroxyurethanes obtained for different types of applications.

To conclude, MILs demonstrated high catalytic activity in both the synthesis of cyclic carbonates and subsequent aminolysis, probably due to their high Lewis acidity. The outcomes of this study demonstrate the versatility of ILs for both steps of the β -hydroxyurethane synthesis.

5. Conclusion

In this thesis, three epoxy reactions, epoxy/dicarboxylic acid, epoxy/anhydride, and epoxy/carbon dioxide, were carried out in the presence of imidazolium ionic liquids (ILs). The obtained results revealed that:

- imidazolium-based IL bearing chloride anion proved to be an efficient catalyst for the epoxy-dicarboxylic acid copolymerization reaction, successfully yielding high epoxy conversion due to its high nucleophile character
- the initiation mechanism of the epoxy-dicarboxylic acid was identified to be via the nucleophilic attack of the IL anion
- the cured epoxy-dicarboxylic acid networks exhibited high thermal stability and good mechanical properties
- the synthesized imidazolium and metal-based ILs (MILs) are efficient accelerators for the epoxy-anhydride copolymerization reaction and can initiate the polyesterification reaction at low temperatures (60-80 °C) due to the enhanced Lewis acidic character
- the initiation mechanism induced by MILs was found to occur via multiple pathways, the imidazole, the counter anion, and the polyesterification routes.
- the crosslinked epoxy-anhydride networks using MILs showed the high crosslink density (3.8 - 5.5 mmol/cm³), high glass transition temperature (up to 171 °C), and excellent thermal stability
- the imidazolium-based ILs, especially MILs effectively catalyzed the epoxy-CO₂ cycloaddition reaction resulting in high yields of cyclic carbonates under mild conditions
- the cycloaddition mechanism between CO₂ and epoxy follows the anionic initiation of the chloride anion of BMIMCl
- the cyclic carbonates reacted with butylamine and successfully delivered β -hydroxyurethane isomers without the use of an additional catalyst in this step

In summary, this thesis highlights the versatility of both metal and non-metal based ILs showcasing their catalytic, initiating and additive effects in various multidisciplinary routes of epoxy reaction pathways.

Publications

Publications included in this thesis:

1. **M. Rebei**, A. Mahun, Z. Walterová, O. Trhlíková, R. K. Donato, H. Beneš. (2022). VOC-free tricomponent reaction platform for epoxy network formation mediated by a recyclable ionic liquid. *Polymer Chemistry* (13), 5380–5388 (IF= 5.364)
2. **M. Rebei**, O. Kočková, M. Řehák, S. Abbrent, A. Vykydalová, J. Honzíček, P. Ecorchard, H. Beneš. (2024). Accelerating effect of metal ionic liquids for epoxy-anhydride copolymerization. *European Polymer Journal* (212), 113077 <https://doi.org/10.1016/j.eurpolymj.2024.113077> (IF= 6.0)
3. **M. Rebei**, C. Červinka, A. Mahun, P. Ecorchard, J. Honzíček, S. Livi, R. K. Donato, H. Beneš. (2024). Fast carbon dioxide–epoxide cycloaddition catalyzed by metal and metal-free ionic liquids for designing non-isocyanate polyurethanes, *Materials Advances*, <https://doi.org/10.1039/D3MA00852E> (IF=5.0)

Other publications:

4. L. Hanzl, J. Vinklarek, M. Litecká, **M. Rebei**, H. Beneš, A. Eisner, T. Míkysek, A. Krejčova, J. Honzíček. Vanadium-containing ionic liquids derived from complexes of modified edta as catalysts of ring-opening polymerization. *Inorganic Chemistry* (IF=4.6) - *Submitted*.

Conference contributions

The results of my PhD study were presented at four international conferences:

1. **M. Rebei**, A. Mahun, R. K. Donato, P. Ecorchard, S. Livi, H. Beneš.
Ionic liquid-catalyzed CO₂-epoxy reaction – a sustainable route to bio-based thermosets (Presentation).
19th International Conference on Renewable Resources & Biorefineries, Riga, Latvia (31/05-02/06/2023)
2. **M. Rebei**, A. Mahun, Z. Walterová, O. Trhlíková, R. K. Donato, H. Beneš.
Ionic liquid-induced formation of bio-sourced epoxy network (Presentation).
XII. Czech-Slovak Polymer conference, Třešť, Czech Republic (03/10-06/10/2022).
3. **M. Rebei**, A. Mahun, R.K. Donato, H. Beneš.
Ionic liquid-catalyzed step growth reaction between difunctional epoxy and dicarboxylic compounds (Poster).
EPF European Polymer Congress, Prague, Czech Republic (26/06-02/07/2022).
4. **M. Rebei**, C. Červinka, A. Mahun, J. Honzíček, P. Ecorchard, H. Beneš.
Metal-free and metal-based ionic liquids as catalysts towards fast carbon dioxide-epoxide cycloaddition: a green approach to non-isocyanate polyurethanes (Poster).
Short Course on Nanostructured Polymer Materials, Lodz, Poland (24/08-28/08/2023).

Grants and projects

Marwa Rebei acknowledges the Charles University Grant Agency (GAUK No. 413022) for financial support of the project titled “Ionic liquid assisted CO₂ fixation - a way towards fully bio-based thermosets” (2022-2023).

Appendices: Publications included in this thesis

1. **M. Rebei**, A. Mahun, Z. Walterová, O. Trhlíková, R. K. Donato, H. Beneš, VOC-free tricomponent reaction platform for epoxy network formation mediated by a recyclable ionic liquid, *Polym. Chem.*, 13 (2022) 5380–5388.
2. **M. Rebei**, O. Kočková, M. Řehák, S. Abbrent, A. Vykydalová, J. Honzíček, P. Ecorchard, H. Beneš. (2024). Accelerating effect of metal ionic liquids for epoxy-anhydride copolymerization. *Eur. Polym. J.*, 212 (2024) 113077.
3. **M. Rebei**, C. Červinka, A. Mahun, P. Ecorchard, J. Honzíček, S. Livi, R. K. Donato, H. Beneš, Fast carbon dioxide–epoxide cycloaddition catalyzed by metal and metal-free ionic liquids for designing non-isocyanate polyurethanes, *Mater. Adv.*, (2024), Advance Article.

References

- [1] M. Zhi, Q. Liu, H. Chen, X. Chen, S. Feng, Y. He, Thermal Stability and Flame Retardancy Properties of Epoxy Resin Modified with Functionalized Graphene Oxide Containing Phosphorus and Silicon Elements, *ACS Omega*. 4 (2019) 10975–10984. <https://doi.org/10.1021/acsomega.9b00852>.
- [2] X. Zhang, X. Lu, L. Qiao, L. Jiang, T. Cao, Y. Zhang, Developing an epoxy resin with high toughness for grouting material via co-polymerization method, *E-Polymers*. 19 (2019) 489–498. <https://doi.org/10.1515/epoly-2019-0052>.
- [3] F.L. Jin, X. Li, S.J. Park, Synthesis and application of epoxy resins: A review, *J. Ind. Eng. Chem.* 29 (2015) 1–11. <https://doi.org/10.1016/j.jiec.2015.03.026>.
- [4] A. Fantoni, T. Koch, S. Baudis, R. Liska, Synthesis and Characterization of Homogeneous Epoxy Networks: Development of a Sustainable Material Platform Using Epoxy-Alcohol Polyaddition, *ACS Appl. Polym. Mater.* (2022). <https://doi.org/10.1021/acsapm.2c01728>.
- [5] A. Shundo, S. Yamamoto, K. Tanaka, Network Formation and Physical Properties of Epoxy Resins for Future Practical Applications, *JACS Au*. 2 (2022) 1522–1542. <https://doi.org/10.1021/jacsau.2c00120>.
- [6] B. Ellis, *Chemistry and Technology of Epoxy Resins*, (1993), 1st ed.
- [7] M. Döring, U. Arnold, Polymerization of epoxy resins initiated by metal complexes, *Polym. Int.* 58 (2009) 976–988. <https://doi.org/10.1002/pi.2618>.
- [8] S. Dagorne, F. Le Bideau, D. Ryzhakov, G. Printz, B. Jacques, S. Messaoudi, F. Dumas, Organo-Catalyzed/Initiated Ring Opening Co-Polymerization of Cyclic Anhydrides and Epoxides: an Emerging Story, *Sci. Twent. Century*. (2013) 547–563. <https://doi.org/10.4324/9781315079097-35>.
- [9] N.G. Jaques, J.J. Pereira Barros, I. Dayane dos Santos Silva, M. Popp, J. Kolbe, R.M. Ramos Wellen, New approaches of curing and degradation on epoxy/eggshell composites, *Compos. Part B Eng.* 196 (2020). <https://doi.org/10.1016/j.compositesb.2020.108125>.
- [10] C. Ding, A.S. Matharu, Recent developments on biobased curing agents: A review of their preparation and use, *ACS Sustain. Chem. Eng.* 2 (2014) 2217–2236. <https://doi.org/10.1021/sc500478f>.
- [11] R.L. Pérez, C.E. Ayala, M.M. Opiri, A. Ezzir, G. Li, I.M. Warner, Recycling Thermoset Epoxy Resin Using Alkyl-Methyl-Imidazolium Ionic Liquids as Green Solvents, *ACS Appl. Polym. Mater.* 3 (2021) 5588–5595. <https://doi.org/10.1021/acsapm.1c00896>.
- [12] E. Sklavounos, J.K.J. Helminen, L. Kyllönen, I. Kilpeläinen, A.W.T. King, Ionic Liquids: Recycling, *Encycl. Inorg. Bioinorg. Chem.* (2016) 1–16. <https://doi.org/10.1002/9781119951438.eibc2451>.
- [13] N. Kaur, Ionic liquid: An efficient and recyclable medium for the synthesis of fused six-membered oxygen heterocycles, *Synth. Commun.* 49 (2019) 1679–1707. <https://doi.org/10.1080/00397911.2019.1568149>.
- [14] O.I. Sidorov, Y.S. Vygodskii, E.I. Lozinskaya, Y.M. Milekhin, A.A. Matveev, T.P. Poisova, F. V. Ferapontov, V. V. Sokolov, Ionic liquids as curing catalysts for epoxide-containing compositions, *Polym. Sci. - Ser. D*. 10 (2017) 134–142. <https://doi.org/10.1134/S1995421217020174>.
- [15] P. Migowski, P. Lozano, J. Dupont, Imidazolium Based Ionic Liquid-Phase Green Catalytic Reactions, *Green Chem.* (2023) 1237–1260. <https://doi.org/10.1039/d2gc04749g>.
- [16] H. Mąka, T. Szychaj, K. Kowalczyk, Imidazolium and deep eutectic ionic liquids as

- epoxy resin crosslinkers and graphite nanoplatelets dispersants, *J. Appl. Polym. Sci.* 131 (2014). <https://doi.org/10.1002/app.40401>.
- [17] J. Lu, F. Yan, J. Texter, Advanced applications of ionic liquids in polymer science, *Prog. Polym. Sci.* 34 (2009) 431–448. <https://doi.org/10.1016/j.progpolymsci.2008.12.001>.
- [18] M. Koel, Physical and Chemical Properties of Ionic Liquids Based on the Dialkylimidazolium Cation, *Proc. Est. Acad. Sci. Chem.* 49 (2000) 145–155. http://www.kirj.ee/public/va_ke/s00-3-ke.htm.
- [19] A. Efimova, G. Hubrig, P. Schmidt, Thermal stability and crystallization behavior of imidazolium halide ionic liquids, *Thermochim. Acta.* 573 (2013) 162–169. <https://doi.org/10.1016/j.tca.2013.09.023>.
- [20] F. Endres, S. Zein El Abedin, Air and water stable ionic liquids in physical chemistry, *Phys. Chem. Chem. Phys.* 8 (2006) 2101–2116. <https://doi.org/10.1039/b600519p>.
- [21] A.I. Leonov, R.J. J, Epoxy Polymers New Materials and Innovations, n.d.
- [22] M. Savla, I. Skeist, Epoxy Resins., *High Polym.* 29 (1977) 582–641. <https://doi.org/10.1108/eb020211>.
- [23] Y. Sarazin, J.F. Carpentier, Discrete Cationic Complexes for Ring-Opening Polymerization Catalysis of Cyclic Esters and Epoxides, *Chem. Rev.* 115 (2015) 3564–3614. <https://doi.org/10.1021/acs.chemrev.5b00033>.
- [24] A.L. Brocas, C. Mantzaridis, D. Tunc, S. Carlotti, Polyether synthesis: From activated or metal-free anionic ring-opening polymerization of epoxides to functionalization, *Prog. Polym. Sci.* 38 (2013) 845–873. <https://doi.org/10.1016/j.progpolymsci.2012.09.007>.
- [25] J. Park, Y. Yu, J.W. Lee, B.S. Kim, Anionic Ring-Opening Polymerization of a Functional Epoxide Monomer with an Oxazoline Protecting Group for the Synthesis of Polyethers with Carboxylic Acid Pendants, *Macromolecules.* 55 (2022) 5448–5458. <https://doi.org/10.1021/acs.macromol.2c00761>.
- [26] J. Herzberger, K. Niederer, H. Pohlitz, J. Seiwert, M. Worm, F.R. Wurm, H. Frey, Polymerization of ethylene oxide, propylene oxide, and other alkylene oxides: Synthesis, novel polymer architectures, and bioconjugation, *Chem. Rev.* 116 (2016) 2170–2243. <https://doi.org/10.1021/acs.chemrev.5b00441>.
- [27] R.-M. Wang, S.-R. Zheng, Y.-P. Zheng, Matrix materials, *Polym. Matrix Compos. Technol.* (2011) 101–548. <https://doi.org/10.1533/9780857092229.1.101>.
- [28] H. Sukanto, W.W. Raharjo, D. Ariawan, J. Triyono, M. Kaavesina, Epoxy resins thermosetting for mechanical engineering, *Open Eng.* 11 (2021) 797–814. <https://doi.org/10.1515/eng-2021-0078>.
- [29] C.W.M. Anshu M. Gupta, No Title, *J. Polym. Sci. B Polym. Phys.* 28 (1990) 2585–2606. <https://doi.org/https://doi.org/10.1002/polb.1990.090281309>.
- [30] T. Vidil, F. Tournilhac, S. Musso, A. Robisson, T. Vidil, F. Tournilhac, S. Musso, A. Robisson, L. Leibler, Control of reactions and network structures of epoxy thermosets To cite this version : HAL Id : hal-02135163, (2019).
- [31] S. Montserrat, Vitriification and further structural relaxation in the isothermal curing of an epoxy resin, *J. Appl. Polym. Sci.* 44 (1992) 545–554. <https://doi.org/https://doi.org/10.1002/app.1992.070440319>.
- [32] R. Hayes, G.G. Warr, R. Atkin, Structure and Nanostructure in Ionic Liquids, *Chem. Rev.* 115 (2015) 6357–6426. <https://doi.org/10.1021/cr500411q>.
- [33] J.P. Hallett, T. Welton, Room-temperature ionic liquids: Solvents for synthesis and catalysis. 2, *Chem. Rev.* 111 (2011) 3508–3576. <https://doi.org/10.1021/cr1003248>.
- [34] S.K. Singh, A. Singh, Effect of Acidity of Ionic Liquids on Hydrogen Bonding Interaction between Ionic Liquids and Lignin Monomers, *ChemistrySelect.* 3 (2018)

- 3570–3574. <https://doi.org/10.1002/slct.201800037>.
- [35] Y. Cao, T. Mu, Comprehensive investigation on the thermal stability of 66 ionic liquids by thermogravimetric analysis, *Ind. Eng. Chem. Res.* 53 (2014) 8651–8664. <https://doi.org/10.1021/ie5009597>.
- [36] Y. Qiao, W. Ma, N. Theyssen, C. Chen, Z. Hou, Temperature-Responsive Ionic Liquids: Fundamental Behaviors and Catalytic Applications, *Chem. Rev.* 117 (2017) 6881–6928. <https://doi.org/10.1021/acs.chemrev.6b00652>.
- [37] C. Dai, J. Zhang, C. Huang, Z. Lei, Ionic Liquids in Selective Oxidation: Catalysts and Solvents, *Chem. Rev.* 117 (2017) 6929–6983. <https://doi.org/10.1021/acs.chemrev.7b00030>.
- [38] M.S. Fedoseev, M.S. Gruzdev, L.F. Derzhavinskaya, 1-Butyl-3-Methylimidazolium Salts As New Catalysts To Produce Epoxy-Anhydride Polymers With Improved Properties, *Int. J. Polym. Sci.* 2014 (2014). <https://doi.org/10.1155/2014/607341>.
- [39] C. Giri, S.E. Sisk, L. Reisman, I. Kammakakam, J.E. Bara, K.N. West, B.D. Rabideau, P.A. Rugar, Anionic Ring-Opening Polymerizations of N-Sulfonylaziridines in Ionic Liquids, *Macromolecules.* 55 (2022) 623–629. <https://doi.org/10.1021/acs.macromol.1c01885>.
- [40] S. Ding, M. Radosz, Y. Shen, Ionic liquid catalyst for biphasic atom transfer radical polymerization of methyl methacrylate, *Macromolecules.* 38 (2005) 5921–5928. <https://doi.org/10.1021/ma050093a>.
- [41] R. Ratti, Ionic Liquids: Synthesis and Applications in Catalysis, *Adv. Chem.* 2014 (2014) 1–16. <https://doi.org/10.1155/2014/729842>.
- [42] M. David, Applications of ionic liquids in polymer science and technology, 2015. <https://doi.org/10.1007/978-3-662-44903-5>.
- [43] M. Perchacz, L. Matějka, R. Konefał, L. Seixas, S. Livi, J. Baudoux, H. Beneš, R.K. Donato, Self-Catalyzed Coupling between Brønsted-Acidic Imidazolium Salts and Epoxy-Based Materials: A Theoretical/Experimental Study, *ACS Sustain. Chem. Eng.* 7 (2019) 19050–19061. <https://doi.org/10.1021/acssuschemeng.9b04810>.
- [44] F.C. Binks, G. Cavalli, M. Henningsen, B.J. Howlin, I. Hamerton, Investigating the mechanism through which ionic liquids initiate the polymerisation of epoxy resins, *Polymer (Guildf).* 139 (2018) 163–176. <https://doi.org/10.1016/j.polymer.2018.01.087>.
- [45] A.P.A. Carvalho, D.F. Santos, B.G. Soares, Epoxy/imidazolium-based ionic liquid systems: The effect of the hardener on the curing behavior, thermal stability, and microwave absorbing properties, *J. Appl. Polym. Sci.* 137 (2020) 1–11. <https://doi.org/10.1002/app.48326>.
- [46] F.D. Bobbink, D. Vasilyev, M. Hulla, S. Chamam, F. Menoud, G. Laurency, S. Katsyuba, P.J. Dyson, Intricacies of Cation-Anion Combinations in Imidazolium Salt-Catalyzed Cycloaddition of CO₂ into Epoxides, *ACS Catal.* 8 (2018) 2589–2594. <https://doi.org/10.1021/acscatal.7b04389>.
- [47] A. Sainz Martinez, C. Hauzenberger, A.R. Sahoo, Z. Csendes, H. Hoffmann, K. Bica, Continuous Conversion of Carbon Dioxide to Propylene Carbonate with Supported Ionic Liquids, *ACS Sustain. Chem. Eng.* 6 (2018) 13131–13139. <https://doi.org/10.1021/acssuschemeng.8b02627>.
- [48] P.P. Pescarmona, Cyclic carbonates synthesised from CO₂: Applications, challenges and recent research trends, *Curr. Opin. Green Sustain. Chem.* 29 (2021) 100457. <https://doi.org/10.1016/j.cogsc.2021.100457>.
- [49] C. Cadena, J.L. Anthony, J.K. Shah, T.I. Morrow, J.F. Brennecke, E.J. Maginn, Why is CO₂ so Soluble in Imidazolium-Based Ionic Liquids?, *J. Am. Chem. Soc.* 126 (2004) 5300–5308. <https://doi.org/10.1021/ja039615x>.
- [50] Y. Marcus, The Solubility Parameter of Carbon Dioxide and Its Solubility in Ionic

- Liquids, *J. Solution Chem.* 48 (2019) 1025–1034. <https://doi.org/10.1007/s10953-018-0816-y>.
- [51] L. Xia, S. Liu, H. Pan, Prediction of the solubility of CO₂ in imidazolium ionic liquids based on selective ensemble modelling method, *Processes*. 8 (2020) 1–14. <https://doi.org/10.3390/pr8111369>.
- [52] Y. Fu, Z. Yang, S.M. Mahurin, S. Dai, D. en Jiang, Ionic liquids for carbon capture, *MRS Bull.* 47 (2022) 395–404. <https://doi.org/10.1557/s43577-022-00315-4>.
- [53] Y. Lee, D. Penley, A. Klemm, W. Dean, B. Gurkan, Deep Eutectic Solvent Formed by Imidazolium Cyanopyrrolide and Ethylene Glycol for Reactive CO₂ Separations, (2020). <https://doi.org/10.1021/acssuschemeng.0c07217>.
- [54] M. Liu, X. Wang, Y. Jiang, J. Sun, M. Arai, Hydrogen bond activation strategy for cyclic carbonates synthesis from epoxides and CO₂ : current state-of-the-art of catalyst development and reaction analysis, *Catal. Rev.* 61 (2019) 214–269. <https://doi.org/10.1080/01614940.2018.1550243>.
- [55] X. Yang, Q. Zou, T. Zhao, P. Chen, Z. Liu, F. Liu, Q. Lin, Deep Eutectic Solvents as Efficient Catalysts for Fixation of CO₂ to Cyclic Carbonates at Ambient Temperature and Pressure through Synergetic Catalysis, (2021). <https://doi.org/10.1021/acssuschemeng.1c03187>.
- [56] J. Peng, S. Wang, H.J. Yang, B. Ban, Z. Wei, L. Wang, B. Lei, Highly efficient fixation of carbon dioxide to cyclic carbonates with new multi-hydroxyl bis-(quaternary ammonium) ionic liquids as metal-free catalysts under mild conditions, *Fuel*. 224 (2018) 481–488. <https://doi.org/10.1016/j.fuel.2018.03.119>.
- [57] W. Cheng, Q. Su, J. Wang, J. Sun, F.T.T. Ng, Ionic liquids: The synergistic catalytic effect in the synthesis of cyclic carbonates, *Catalysts*. 3 (2013) 878–901. <https://doi.org/10.3390/catal3040878>.
- [58] M.H. Anthofer, M.E. Wilhelm, M. Cokoja, M. Drees, W.A. Herrmann, F.E. Kühn, Hydroxy-functionalized imidazolium bromides as catalysts for the cycloaddition of CO₂ and epoxides to cyclic carbonates, *ChemCatChem*. 7 (2015) 94–98. <https://doi.org/10.1002/cctc.201402754>.
- [59] Y. Li, B. Dominelli, R.M. Reich, B. Liu, F.E. Kühn, Bridge-functionalized bisimidazolium bromides as catalysts for the conversion of epoxides to cyclic carbonates with CO₂, *Catal. Commun.* 124 (2019) 118–122. <https://doi.org/10.1016/j.catcom.2019.03.012>.
- [60] Y. Yang, Y. Guo, C. Gao, M. North, J. Yuan, H. Xie, Q. Zheng, Fabrication of Carboxylic Acid and Imidazolium Ionic Liquid Functionalized Porous Cellulosic Materials for the Efficient Conversion of Carbon Dioxide into Cyclic Carbonates, *ACS Sustain. Chem. Eng.* 11 (2023) 2634–2646. <https://doi.org/10.1021/acssuschemeng.2c06976>.
- [61] Y. Wang, J. Nie, C. Lu, F. Wang, C. Ma, Z. Chen, G. Yang, Imidazolium-based polymeric ionic liquids for heterogeneous catalytic conversion of CO₂ into cyclic carbonates, *Microporous Mesoporous Mater.* 292 (2020) 109751. <https://doi.org/10.1016/j.micromeso.2019.109751>.
- [62] A. Rehman, F. Saleem, F. Javed, A. Ikhlaq, S. Waqas, A. Harvey, Recent advances in the synthesis of cyclic carbonates via CO₂ cycloaddition to epoxides, *J. Environ. Chem. Eng.* 9 (2021) 105113. <https://doi.org/10.1016/j.jece.2021.105113>.
- [63] F. Li, L. Xiao, C. Xia, B. Hu, Chemical fixation of CO₂ with highly efficient ZnCl₂/[BMIm]Br catalyst system, *Tetrahedron Lett.* 45 (2004) 8307–8310. <https://doi.org/10.1016/j.tetlet.2004.09.074>.
- [64] J.-I. Yu, H.-Y. Ju, K.-H. Kim, D.-W. Park, Cycloaddition of carbon dioxide to butyl glycidyl ether using imidazolium salt ionic liquid as a catalyst, *Korean J. Chem. Eng.*

- 27 (2010) 446–451. <https://doi.org/10.1007/s11814-010-0074-1>.
- [65] S. Wang, Z. Zhu, D. Hao, T. Su, C. Len, W. Ren, H. Lü, Synthesis cyclic carbonates with BmimCl-based ternary deep eutectic solvents system, *J. CO2 Util.* 40 (2020) 101250. <https://doi.org/10.1016/j.jcou.2020.101250>.
- [66] N. Si, Room-temperature ionic liquids: a novel versatile lubricant, (2001) 2244–2245. <https://doi.org/10.1039/b106935g>.
- [67] B.G. Soares, S. Livi, J. Duchet-Rumeau, J.F. Gerard, Synthesis and characterization of epoxy/MCDEA networks modified with imidazolium-based ionic liquids, *Macromol. Mater. Eng.* 296 (2011) 826–834. <https://doi.org/10.1002/mame.201000388>.
- [68] P. Maksym, M. Tarnacka, A. Dzienia, K. Matuszek, A. Chrobok, K. Kaminski, M. Paluch, Enhanced Polymerization Rate and Conductivity of Ionic Liquid-Based Epoxy Resin, *Macromolecules.* 50 (2017) 3262–3272. <https://doi.org/10.1021/acs.macromol.6b02749>.
- [69] Z. Jiang, Q. Wang, L. Liu, Y. Zhang, F. Du, A. Pang, Dual-Functionalized Imidazolium Ionic Liquids as Curing Agents for Epoxy Resins, *Ind. Eng. Chem. Res.* 59 (2020) 3024–3034. <https://doi.org/10.1021/acs.iecr.9b06574>.
- [70] R. Sonnier, L. Dumazert, S. Livi, T.K.L. Nguyen, J. Duchet-Rumeau, H. Vahabi, P. Laheurte, Flame retardancy of phosphorus-containing ionic liquid based epoxy networks, *Polym. Degrad. Stab.* 134 (2016) 186–193. <https://doi.org/10.1016/j.polymdegradstab.2016.10.009>.
- [71] B.G. Soares, A.A. Silva, J. Pereira, S. Livi, Preparation of epoxy/jeffamine networks modified with phosphonium based ionic liquids, *Macromol. Mater. Eng.* 300 (2015) 312–319. <https://doi.org/10.1002/mame.201400293>.
- [72] R. Henriques, B.G. Soares, S. Livi, From Epoxy Prepolymers to Tunable Epoxy – Ionic Liquid Networks : Mechanistic Investigation and Thermo-Mechanical Properties, (2023) 3–10. <https://doi.org/10.1021/acsapm.3c00551>.
- [73] L. Orduna, I. Razquin, I. Otaegi, N. Aranburu, G. Guerrica-Echevarría, Ionic Liquid-Cured Epoxy/PCL Blends with Improved Toughness and Adhesive Properties, *Polymers (Basel).* 14 (2022). <https://doi.org/10.3390/polym14132679>.
- [74] R.R. Henriques, C.P. De Oliveira, R. Stein, K. Pontes, A.A. Silva, B.G. Soares, Dual Role of Magnetic Ionic Liquids as Curing Agents of Epoxy Resin and Microwave-Absorbing Additives, *ACS Appl. Polym. Mater.* 4 (2022) 1207–1217. <https://doi.org/10.1021/acsapm.1c01584>.
- [75] M. Rebei, A. Mahun, Z. Walterová, O. Trhlíková, R.K. Donato, H. Beneš, VOC-free tricomponent reaction platform for epoxy network formation mediated by a recyclable ionic liquid, *Polym. Chem.* 13 (2022) 5380–5388. <https://doi.org/10.1039/d2py01031c>.
- [76] M. Rebei, O. Kočková, M. Řehák, S. Abbrent, J. Honzíček, P. Ecorchard, H. Beneš, Accelerating effect of metal ionic liquids for epoxy-anhydride copolymerization, *Eur. Polym. J.* 212 (2024) 1–12. <https://doi.org/10.1016/j.eurpolymj.2024.113077>.
- [77] M. Rebei, C. Červinka, A. Mahun, P. Ecorchard, J. Honzíček, S. Livi, R.K. Donato, H. Beneš, Fast carbon dioxide–epoxide cycloaddition catalyzed by metal and metal-free ionic liquids for designing non-isocyanate polyurethanes (Accepted manuscript), *Mater. Adv.* (2024). <https://doi.org/10.1039/D3MA00852E>.
- [78] A. Gomez-Lopez, F. Elizalde, I. Calvo, H. Sardon, Trends in non-isocyanate polyurethane (NIPU) development, *Chem. Commun.* 57 (2021) 12254–12265. <https://doi.org/10.1039/d1cc05009e>.
- [79] L. Maisonnette, O. Lamarzelle, E. Rix, E. Grau, H. Cramail, Isocyanate-Free Routes to Polyurethanes and Poly(hydroxy Urethane)s, *Chem. Rev.* 115 (2015) 12407–12439. <https://doi.org/10.1021/acs.chemrev.5b00355>.